Development of transparent and flexible field emission display

By

Debasish Ghosh

Doctor of Philosophy

Nagoya Institute of Technology

2013

Dedicated to my beloved parents

Contents

List of Figures

Chapter 1

Chapter 2

Chapter 3

Chapter 4

Chapter 5

List of symbols and acronyms

CRTs	Cathode ray tubes
FPD	Flat panel display
AMOLED	Active-matrix organic light-emitting diode
PET	Polyethylene terephthalate
SWCNT	Single wall carbon nanotube
ACEL	Alternating current electroluminescence devices
OLED	Organic light-emitting diode
FED	Field emission display
LCD	Liquid-crystal display
PDP	Plasma display panel
ELD	Electroluminescent display
DLP	Digital Light Processing
IMOD	Interferometric modulator display
QLED	Quantum dot display
SED	Surface-conduction electron-emitter display
NED	Nano-emissive display
FE	Field emission

FEE	Field electron emitter
F-N	Fowler-Nordheim
J	Current density
A	Constant of F-N plot
B	Constant of F-N plot
E	Electric field
B	Field enhancement factor
Φ	Work function
CNTs	Carbon nanotubes
AUO	AU Optronics Corporation
CNCSs	Conical nanocarbon structures
ZnO	Zinc oxide
DCE	1, 2- dicholoro ethane
PEDOT:PSS	Poly(3,4-ethylenedioxythiophene): poly(styrenesulfonate)
SOG	Spin on glass
FESEM	Field emission scanning electron microscopy
AFM	Atomic force microscopy
RBM	Radial breathing mode

ω	RBM peak frequency
TEM	Transmission electron microscopy
UV-Vis	Ultra violet and visible spectra
kΩ	kilohm
sq	Square
mA	milliampere
A	Ampere
n	nano ampere
V	Volt
μm	micrometer
CaF_2	Calcium fluoride
Au	Gold
ITO	Indium tin oxide
AVO_3	Metavanadate (A= K, Rb and Cs)
nm	nanometer
T	Transmittance
e^-	electron
Pa	Pascal

MWCNT	Multiwall carbon nanotube
PDMS	Polydimethylsiloxane
ml	Milliliter
wt%	Weight percent
conc	Concentration
°C	degree Celsius
min	Minute
h	hour
mg	milligram
rpm	Revolutions per minute
MPa	megapascal
HRTEM	High resolution transmission electron microscopy

List of Tables

Abstract

Transparency and flexibility are key words required for future bendable, lightweight and rollable display device applications. Among various types of displays, field emission displays (FEDs) offer promising advantages such as high brightness, wider viewing angle, less power consumption and very high response time. In this thesis, I focused on the transparent and flexible FEDs which have not been realized yet. To achieve the successful development of transparent and flexible device, fabrication of following major components of FEDs were necessary: (i) electrodes, (ii) electron emitters, and (iii) screen. For the fabrication of electrodes and emitters, nanocarbons and conducting polymer such as single wall carbon nanotubes (SWCNTs), conical nanocarbon structures (CNCSs) and Poly(3,4-ethylenedioxythiophene): poly(styrenesulfonate) (PEDOT:PSS), respectively were employed, because of their high conductivity and good field emission (FE) properties. Finally, by combining those developments with an oxide film as screen, transparent and flexible FEDs were successfully demonstrated. In this dissertation, I will reveal those achievements in detail.

Chapter 1

Introduction

1.1 Background

Displays are electronic devices in which a still or moving object can be focused. Display devices play an important role to convey the information. As pictures and any information composed of several words, display simplifies this information.

For the past 60 years, cathode ray tubes (CRTs) were the most dominant technology devices. The CRTs are major display devices for video applications. CRTs are used in various fields like television sets, computer monitors, automated teller machines, video game machines, video cameras, oscilloscopes and radar displays. CRTs are much simpler than other displays and it has lot of advantages like low manufacturing cost, and to produce high quality images etc. [1]. However, most significant disadvantage of this display is that it is bulky and fragile. In order to overcome these negative aspects, this well-known CRT was replaced by flat panel displays (FPDs) technologies due to their several advantages like thickness, low power consumption and lightweight etc. [2]. These FPDs are widely used in various applications like in laptop screen, mobile screen and so on [3]. The modern FPDs are advantageous over CRTs; the FPDs require small space and it consumes less power compared to CRT.

According to Slikkerveer, a flexible FPDs are constructed of thin (flexible) substrates that can be bent, flexed, conformed, or rolled to a radius of curvature of a few

centimeters without losing functionality. So far, various companies have been trying to commercialize the transparent and flexible displays. Samsung has already demonstrated the model for transparent and flexible active-matrix organic light-emitting diode (AMOLED) screen for mobile device. However, the transparent and flexible display has many components like electrode materials, manufacturing process (roll-to-roll) and suitable phosphor materials etc. and it differs from technology to technology. These components have to optimize in order to realize the transparent and flexible displays. Fig. 1.1.1 demonstrates the features of different FPDs towards the next-generation display devices.

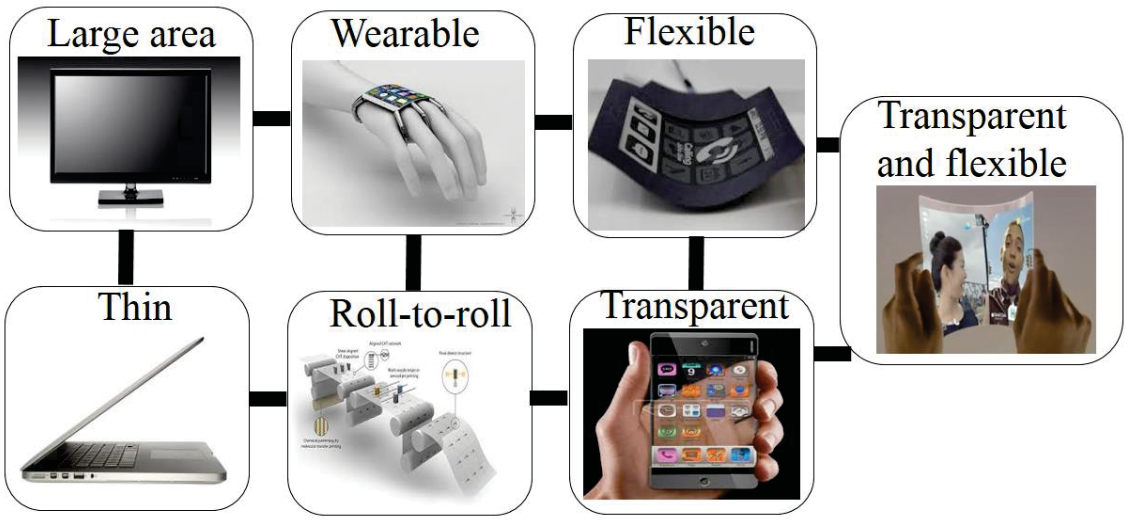

Fig. 1.1 Special feature of flat panel display.

Next-generation FPDs require ultrathin transparent and bendable screen which could be energy-efficient, wearable character and high-resolution etc. The bendable and

transparent screen could be applied in televisions, computers, phones and digital newspaper displays. Such kinds of bendable and transparent screen for different display devices could be the key component for the future electronic devices due to their above mentioned properties.

Various transparent and flexible displays are being studied at length due to their great potential to make major impact in the wide varieties of areas. So far, only few reports have been studied on transparent and flexible displays [4-5] and most of the literature reports focused either on transparency or on the flexibility of the device [6-10].

Recently Jang et al. studied the transparent and flexible plasma display based on organic materials fabricated on polyethylene terephthalate (PET) substrate [11]. Scharge et al. reported the fabrication of SWCNTs based electrode for transparent and flexible alternating current electroluminescent devices (ACEL) [12]. Recently transparent and flexible electrode has been developed for organic light-emitting diode (OLED) displays [13].

Of late FEDs are considered as one of the most promising next-generation FPDs and will solve those drawbacks.

1.2 Various kinds of displays

Display devices are broadly classified into three main categories; Segment

displays, CRTs and FPDs.

1.2.1 Segment display

Segment displays are composed of several illuminated digits to give direct visual of desired symbols, numbers and images etc. Digital numbers, alphanumeric characters can be shown by these kinds of displays. There are several kinds of segment displays like seven-segment display, fourteen-segment display, sixteen-segment display, HD44780 LCD controller. These displays are mainly used in calculators, digital wristwatches, microwave oven and petrol pump displays etc. [14]. However, these displays have been replaced by dot-matrix display.

1.2.2 Dot-matrix display

To represent symbols and images, dot-matrix display is often used in many fields like wristwatch, indicators in railway station, airport and vending machines etc. Dot-matrix displays are in limited resolution.

1.3 Cathode ray tube

CRTs are the very oldest display technology. A CRT is a special kind of vacuum tube containing an electron gun and fluorescent screen in which images are produced when the electron strikes to the fluorescent screen.

In CRTs, the electrons strike at the phosphor material to create image. There are

three main components in CRTs; electron gun, electron beam deflector and the screen (phosphor materials) [15]. The electron gun generates electrons and it accelerates through the anode materials. An extremely low magnetic field was produced through the coil and it adjusts the direction of the electron beam. This electron beam produced a small tiny hole in the phosphor coated screen.

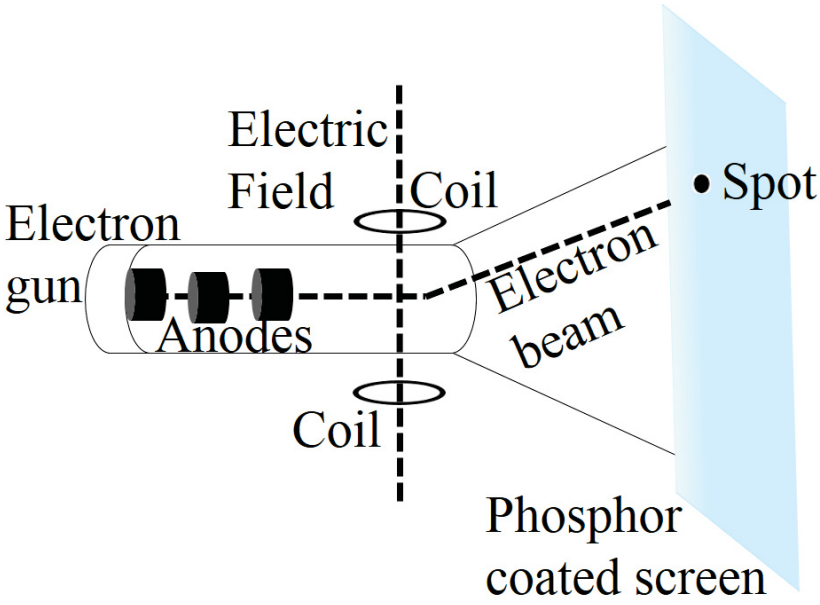

Fig. 1.2 Working principles of cathode ray tube.

This schematic diagram shows only one electron gun that is monochromatic CRTs shown in Fig.1.2. However, future CRTs can produce color images. Although the CRTs are mature technology, there is further room to improve the device performances. Earle et al. considered that 640 by 400 pixels were the high-resolution CRTs display in the year of 1984 [16]. Today's high resolution displays focused 2000 pixels in each

direction. Although the CRTs display are now being replaced by FPDs, but CRTs can use in many areas.

The major advantage of CRTs is that it is cost-effective displays compared to the other displays. As the CRTs technologies are matured, we can use it for longer period of time.

Besides these advantages of CRTs displays, it has several disadvantages. Because of their heavy weight and larger size, this display is very difficult to store in the market. It consumes a lot of power compared to that of other FPDs. As the color of this display is quickly faded out, it must be refreshed in every time in order to keep the screen always bright.

1.4 Flat panel displays

The most common FPDs are organic light-emitting diode (OLED), liquid-crystal display (LCD), plasma display panel (PDP), E-paper, electroluminescent display (ELD), digital light processing (DLP), interferometric modulator display (IMOD), quantum-dot display (QLED), nano-emissive display (NED), and surface-conduction electron-emitter display (SED) etc. The brief discussions of these displays are given below.

1.4.1 Organic light-emitting diode

An OLED consists of four parts. The emissive and the hole transporting layer is

sandwiched between the cathode and anode. The emissive layer is made of organic plastic molecules and most commonly used organic polymer in the emissive layer is polyfluorene. The working principle of OLED is shown here in Fig. 1.3.

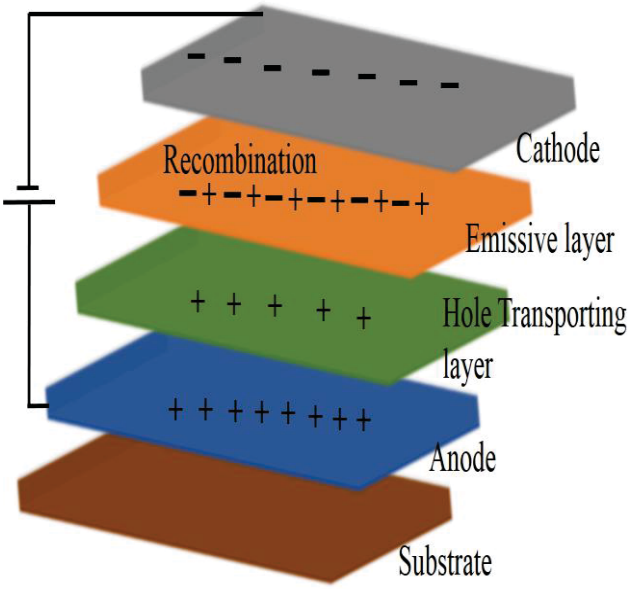

Fig. 1.3 A schematic diagram of organic light-emitting diode.

The hole from the anode and the electron from the cathode are generated by applying a certain voltage. When an electron combines with a hole it drops from high energy state to low energy state and the difference in energy is released as a photon of light. The wavelength of the light is dependent on the energy gap between the emitting materials.

OLED has many advantages over LCD. OLED does not require any backlighting and thus it considers as an energy-efficient device. Moreover, the image quality of OLED

is better than LCD.

OLED can be used in varieties of electronic devices including television screen, computer monitors, and also in portable devices such as mobiles, personal digital assistants (PDAs) etc. This type of display can also be applied to solid state lighting including LED lamp, street lights, traffic and parking lot lights etc.

1.4.2 Liquid-crystal display

LCD is also one kind of FPDs, and it follows the light modulating properties of liquid crystals. Liquid crystals are the substances which exhibit the properties of both solid and liquid. Liquid crystal can be classified into three different categories viz. nematic, smectic, and cholestric depending on the crystal orientation.

This display consumes less power compared to that of OLED. The contrast level of this display is very high and the fabrication cost is also cheap. In LCD, as there is no phosphor used so this display do not suffer from image burning.

Besides these advantages, this display suffers from low visibility, slow response time and low reliability etc.

LCDs are used in wide range of applications such as computer monitors, television, aircraft cockpit displays and besides these it can be used in mobile phones, clocks, gaming devices, and calculator etc.

1.4.3 Quantum-dot display

The nanotechnology based display is quantum dot (QD) display in which quantum dots are used as a replacement of phosphor material. The emitted color from a quantum dot depends on the size of the quantum particles. Different sizes of QDs are arranged by different quantum dots in alternating position and these QDs are excited by electron.

1.4.4 Nano-emissive display

CNT based FEDs are called sometimes by nano-emissive display (NED) by Motorola. They were able to produce a 5 inch. display by growing CNTs on glass substrate.

1.4.5 Surface-conduction electron-emitter display

Surface-conduction electron-emitter display (SED) is also closely related to FEDs technology, where only single electron emitter is used per area rather than multiple electron emitters that are used in FEDs.

1.4.6 E-paper

E-paper is one kind of FPDs, which is designated to follow the appearance of printed ink on paper.

Compared to the other FPDs, it has longer battery life. It consumes less power

as it does not require any kind of backlight. E-paper is readable in the sunlight without affecting the image quality. In spite of this, this display has low refresh rate.

This display can be applied to E-books, gift cards, E-watch, E-newspaper, and touchable pads etc.

1.5 Field emission display

FED is one kind of promising FPDs in which the cathode material is bombard with phosphor materials so as to produce the color image.

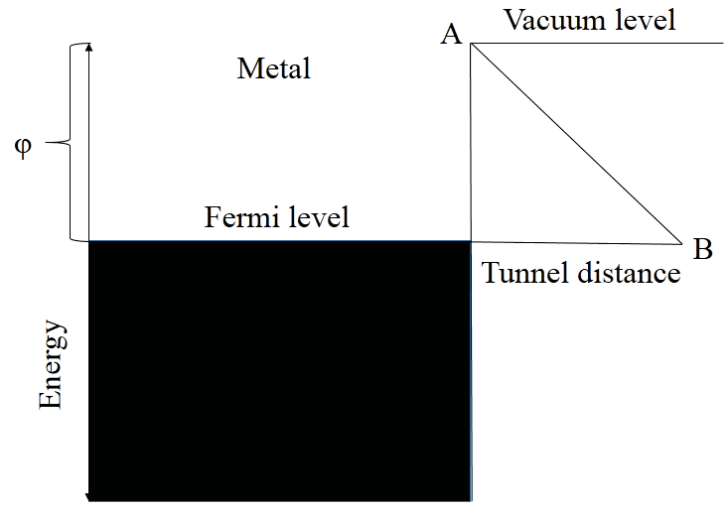

Fig. 1.4 Basics of field emission.

The minimum energy required to remove an electron from the Fermi level to the Vacuum level is called the work function of the material. To excite the electron from the material, electrons should have an energy which exceeds the work function. This can be achieved by different ways like thermal excitation, the absorption of photons etc. Fields

emission differs from these kinds of emissions and instead of gaining the energy, the electrons tunnel through the potential barrier.

Field electron emission describes the extraction of electron from a material using the tunneling effect shown in Fig 1.4. Here the metal can be considered as a conductive substrate filled with electrons which lie below the vacuum level. Generally, the electrons are confined within a conductor. In the presence of certain electric field, the potential energy barrier of the metal surface will be reduced and the electrons easily tunnel through the path AB.

The working principles of FEDs are quite similar to the CRT technology. In case of CRT, only one electron gun has been used to emit electrons to hit the screen. In FEDs, millions of smaller tips have been used as the electron source [17]. In FED, the phosphor materials are the screens in which the images are displayed. This phosphor screen acts as an anode material which receives the electron from the cathode material. The schematic diagram for FEDs is shown in Fig. 1.5. The cathode materials are called the electron guns which emit the electrons. The two electrodes (anode and cathode) are separated by a spacer. In the presence of applied voltage, the emitted electrons from the cathode excite to the phosphor materials and subsequently produce the color image. As there is no heat involved in the FEDs, the emission of electrons are also called cold

cathode electron source.

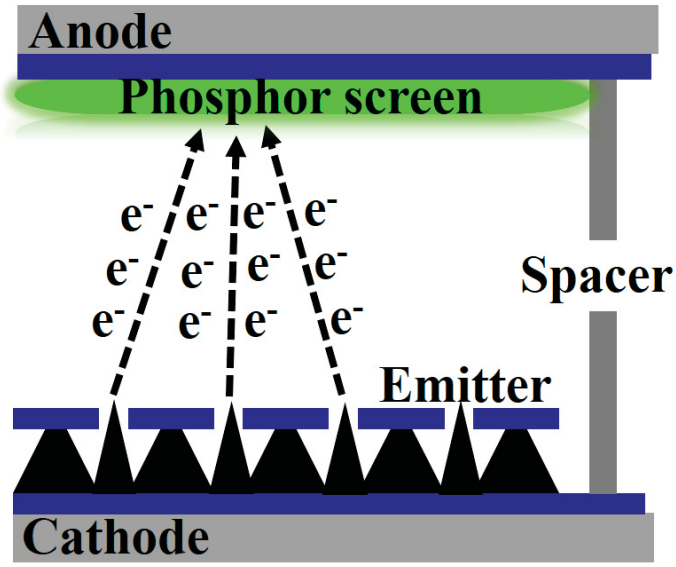

Fig. 1.5 A schematic diagram for FEDs.

The FE experiments followed the Fowler and Nordheim (F-N) plot expressed by the following relation:

$J = A((\beta^2 E^2)/\phi) \exp((-B\phi^{3/2})/\beta E)$,

Where J is the current density and the E is the applied electric field, A and B are two constants and the values of A and B are given below:

$A = 1.56\times10^{-10}\ AV^{-2}eV$

$B = 6.83\times10^{3}\ VeV^{-3/2}\mu m^{-1}$

β is the field enhancement factor and ϕ is the work function of the corresponding material.

The β can be calculated from the slope of the F-N plot and can be expressed as

$\beta = - (B\phi^{3/2})/\text{slope}$.

Nowadays FEDs offer promising advantages for the future low cost flexible devices. Following are the most common advantages of FEDs:

I FEDs have better candidate compared to that of other well-known display devices.

II The thickness and weight is $1/10^{th}$ than that of CRT

III Image can be viewed from any angle without affecting brightness and contrast of the displays.

IV FED requires less power compared to that of other displays.

V The display cost is lower than other displays.

VI FED is suitable under extreme environmental condition.

Due to the above-mentioned advantages, this display can be applied to windshield in cars and airplane, head-up displays in airplane and in the electronic devices including computer screen, video games and for the security application.

Carbon nanotubes (CNTs) due to their sharp emission tip, high aspect ratio, good environmental, thermal and chemical stability etc. are an effective choice for the fabrication of FEDs [18-22]. It can be applied in vast range of applications in material science fields. Taking the advantages of the unique property of CNTs, here in this present dissertation I have fabricated the transparent and flexible FEDs.

1.5.1 Materials used for FEDs

The suitable materials towards FED must offer the possibility of equivalent or improved device performance as well as cost-effective when compared to the other devices. Furthermore, it must have the following characteristics features like high transparency, low sheet resistance, inert in atmospheric condition, and non-toxic etc.

Over the past few years, several kinds of materials have been used in FEDs. Recently, carbon nanofibers (CNF) based field electron emitter (FEE) has been extensively studied at high temperature [23]. The FE properties of aligned metal composite CNF have been reported on copper substrate at room temperature [24].

The most common materials for FEDs are zinc oxide (ZnO) based nanostructures [25], CNTs [26], CNCSs [27], and graphene [28]. Recent research focused on the hybrid structure of graphene and metallic nanowire and graphene with CNTs etc. [29-30]. Among these materials CNTs are known to be very efficient material for FEDs.

The unique properties of the CNTs make them very useful in various fields. CNTs are flexible, and have high young's modulus, high aspect ratio, and unusual electrical properties ranging from metallic to semiconductors depending on their unique quantum mechanical structure [31]. Their electrical conductivity is almost equal to diamond and the mechanical strength is greater than steel [32].

There are many obstacles need to overcome to develop transparent and flexible FEDs. Firstly, plastic substrate must be used to develop the transparent and flexible FEDs, since its glass transition temperature is very low. As a result low temperature fabrication process is essentially required. Secondly, room temperature growth of the carbon nanomaterials onto plastic substrate is needed. Thirdly, there is a need of direct fabrication of the phosphor material onto transparent and flexible substrate. Finally, increase the FE device performances, and FE device performances can be improved by the formation of the hybrid structure onto transparent and flexible substrate.

To realize the transparent and flexible FEDs, the present work has been performed and in this dissertation I will discuss these issues elaborately in the main Chapter.

1.5.2 Current status of FED

The importance of the display devices towards the human society plays a crucial role to receive the information. FED is most promising displays for future FPDs as a successor of CRTs. This FPDs technology has created huge interests in several fields of electronics.

Silicon Video Corporation, Candescent Technologies first started their efforts to develop spindt-type FEDs with molybdenum tips in the year of 1991. However, because of higher accelerating voltage and erosion problems, they remained unsuccessful. In spite

of those above problems, the candescent technologies collaborated with Sony to develop the FEDs in the year of 1998 in Silicon Valley. However, their efforts went in vain developing this display and they filed for Chapter 11 Protection in June 2004. They sold their all assets to the Cannon in August 2004.

Advanced Nanotech, a U.S.A. based company, was also tried to develop the FEDs using diamond dust as an emitter. However, the development was not happened successfully and finally they cancelled their further attempt. Consequently, Advanced Nanotech transferred their technology to Cannon and Cannon too handed over their technology to Toshiba.

Recently, researcher focused on CNT based FED. A prototype model was developed by Motorola in May 2005, and now they have stopped FED related research. Spindt-type FED has been developing by Futaba Corporation since 1990. They developed few smaller screen spindt-type FED. The development shifted again to the CNT based large screen keeping in mind for the production for the present market value.

FE technology was closed down due to the inability to raise the market value in March 2009. However, AU Optronics Corporation (AUO), a Taiwan based company, announced that Sony's FET and FET in Japan had enough scope to develop FED in January 2010. Nikkei reported that AUO plans to start mass production of FED panels in

November 2010. AUO realized that the technology is not matured and their efforts became also unsuccessful.

Recently, Lahiri et al. reported the fabrication of transparent and flexible FEDs based on graphene [33]. Verma et al. fabricated the transparent and flexible FEDs using CNTs and graphene hybrid structure as a cathode material [28]. Arif et al. fabricated transparent and flexible FEDs based on metallic nanowire and graphene based hybrid structure [27]. Hwang et al. reported the fabrication of transparent and flexible FEDs based on vertical ZnO nanowire/graphene based hybrid structure [34].

1.6 Purpose and organization of dissertation

Generally, FED has been fabricated on glass substrate. This gives a major setback in terms of weight, reliability, and cost. Due to the fragile nature of this display, it is difficult to use them in environments. In order to reduce the weight and thickness of the display and makes them durable, a shift in technology is required using transparent and flexible substrate. The substrates for such displays are heat-sensitive polymer. Since these substrates are transparent and flexible, the display fabricated on such substrates can potentially be rolled or folded like paper. This revolutionizes a new technology area which can be used in variety of low cost applications like automotive displays, mobiles, smart cards etc. Next-generation transparent and flexible FEDs could be helpful to fulfill

those.

To realize the transparent and flexible FEDs, in the present dissertation, I have decided to fabricate this display and successfully achieved my object.

In Chapter 1, the background, a brief description of different displays and the purpose of this thesis are described in detail.

Chapter 2 describes the dispersion of SWCNTs in 1, 2- dicholoro ethane (DCE), and that the fabrication of transparent, conductive and flexible thin film using SWCNTs solution by spray coating on polymer substrate. By using this SWCNTs film as both electrode and electron emitter, SWCNT-based transparent and flexible electron emitter with transmittance higher than 86% at 550 nm was first demonstrated.

Chapter 3 describes the development of the transparent and flexible anode phosphor screen for FED devices. For this purpose, Cesium Metavanadate (CsVO3) was coated on the SWCNTs film on arylite substrate at room temperature. By combining the SWCNT emitter developed in Chapter 2 with this phosphor screen, transparent and flexible FED was fabricated for the first time.

Chapter 4 describes the improvement in the conductivity for the cathode material using SWCNTs and conducting polymer PEDOT:PSS based hybrid structure. The FE properties of the PEDOT:PSS/SWCNTs hybrid structure are dramatically increased than

either PEDOT:PSS or SWCNTs material due to the emission properties of the SWCNTs material and the high conductivity of the PEDOT:PSS film. It is thus believed that the high conductivity of PEDOT:PSS material helps the electron emitter SWCNTs, by continuous supply of electrons. Thus, the SWCNTs-based transparent and flexible field electron emitter with transmittance higher than 90% in the visible light region was achieved for the first time.

Chapter 5 deals with the improvement in the transparency and FE properties using the CNCSs fabricated directly on transparent and flexible nafion substrate by the irradiation with Ne^+ ions for short irradiation time (10 sec). The enhanced FE properties of the CNCSs and the transmittance higher than 90% in the visible light region can be achieved by simply coating a very small amount of SWCNTs dispersed solution on the CNCSs surfaces. Thus, the importance of the combination of SWCNTs and CNCSs was first demonstrated for the development of transparent and flexible FEDs. Both SWCNTs and CNCSs acted as an effective FEE towards the development of transparent and flexible FEDs.

Chapter 6 summarizes the present thesis and also focused on the future research work.

1.7 References

[1] P. J. Slikkerveer, Inf. Disp. **3**, 20-24 (2003).

[2] William A. MacDonald, J. Mater. Chem **14**, 4-10 (2004).

[3] S. Ju, J. Li, J. Liu, P.-C. Chen, Y.-G. Ha, F. Ishikawa, H. Chang, C. Zhou, A. Facchetti, D. B. Janes, and Tobin J. Marks, Nano Lett., **8**, 997-1004 (2008).

[4] J. Zhang, C. Wang, and C. Zhou, ACS Nano. **6**, 7412-7419 (2012).

[5] J. Lewis, S. Grego, B. Chalamala, E. Vick, and D. Temple, Appl. Phys. Lett. **85**, 3450-3452 (2004).

[6] X. Liu, Y.-Z. Long, L. Liao, X. Duan, and Z. Fan, ACS Nano, **6**, 1888-1890 (2012).

[7] W.-S. Song, H.-N. Choi, Y.-S. Kim and H. Yang, J. Mater. Chem **20**, 6929-6934 (2010).

[8] A. B. Chwang, M. Hack, J. J. Brown, J. Soc. Inf. Display, **13**, 481-486, (2005).

[9] J. Jang, Materials Today, **9**, 46-52 (2006).

[10] S. Takamatsu, T. Takahata, M. Muraki, E. Iwase, K. Matsumoto and I. Shimoyama, J. Micromech. Microeng. **20**, 075017-6 (2010).

[11] C. Jang, K. Kim, and K. C. Choi, IEEE Electron Device Lett., **33**, 74-76 (2012).

[12] Christian Schrage and Stefan Kaskel, ACS Appl. Mater. Interfaces **1**, 1640-1644 (2009).

[13] K.-H. Choi, H.-J. Nam, J.-A. Jeong, S.-W. Cho, H.-K. Kim, J.-W. Kang, D.-G.

Kim, and W.-J. Cho, Appl. Phys. Lett. **92**, 223302-3 (2008).

[14] P. P. Ray, International Journal of Computer Trends and Technology, **2**, 161-166, (2011).

[15] S. Larach, and A. E. Hardy, Proceedings of the IEEE, **61**, 915-926 (1973).

[16] A. S. Earle, Taking a closer look at the RGB monitor. PC Magazine, **3**, 145-150 (1984).

[17] A G. Rinzler, J. H. Hafner, P. Nikolaev, L. Lou, S. G. Kim, D. Tomimek, P. Nordlander, D. T. Colbert, R. E. Smalley, Science, **269**, 1550-1553 (1995).

[18] M. S. Wang, L.-M. Peng, J. Y. Wang, C. H. Jin, and Q. Chen, J. Phys. Chem. B **110**, 9397-9402 (2006).

[19] H. Xia, Q. Wang, and G. Qiu, Chem. Mater. **15**, 3879-3886 (2003).

[20] K. A. Dean, and Babu R. Chalamala, Appl. Phys. Lett. **75**, 3017-3019 (1999).

[21] B. Frank, A. Rinaldi, R. Blume, R. Schlogl, and D. S. Su, Chem. Mater. **22**, 4462-4470 (2010).

[22] L. A.-Abramovich, M. Reches, V. L. Sedman, S. Allen, S. J. B. Tendler, and E. Gazit, Langmuir **22**, 1313-1320 (2006).

[23] P. Ghosh, M. Z. Yusop, D. Ghosh, T. Soga, T. Jimbo, S. Hashimoto, S. Ohashi, and M. Tanemura, Jpn. J. Appl. Phys, **50**, 01AF09-4 (2011)

[24]. P. Ghosh, M. Z. Yusop, D. Ghosh, A. Hayashi, Y. Hayashi, and M. Tanemura, Chem. Commun, **47**, 4820-4822 (2011).

[25] Y. H. Yang, B. Wang, N. S. Xu, and G. W. Yang, Appl. Phys. Lett. **84**, 043108-3 (2006).

[26] N. Liu, G. Fang, W. Zeng, H. Zhou, H. Long and X. Zhao, J. Mater. Chem., **22**, 3478-3484 (2012).

[27] P. Ghosh, M. Z. Yusop, S. Satoh, M. Subramanian, A. Hayashi, Y. Hayashi, and M. Tanemura, J. Am. Chem. Soc. **132**, 4034-4035 (2010).

[28] D. Ye, S. Moussa, J. D. Ferguson, A. A. Baski, and M. S. E.-Shall, Nano Lett. **12**, 1265-1268 (2012).

[29] M. Arif, K. Heo, B. Y. Lee, J. Lee, D. H Seo, S. Seo, J. Jian, and S. Hong, Nanotechnology **22**, 355709-7 (2011).

[30] I. Lahiri, V. P. Verma, W. Choi, Carbon. **49**, 1614-1619 (2011).

[31] M. S. Dresselhaus, G. Dresselhaus, J. C. Charlier and E. Hernandez, Phil. Trans. R. Soc. Lond. A, **362**, 2065-2098 (2004).

[32] Q. Yi, X. Dai, J. Zhao,Y. Sun,Y. Lou, X. Su, Q. Li, B. Sun,H. Zheng, M. Shen, Q. Wang, and G. Zou, Nanoscale, **5**, 6923-6927 (2013).

[33] V. P. Verma, S. Das, I. Lahiri, W. Choi, Appl. Phys. Lett. **96**, 203108-3 (2010).

[34] J. O. Hwang, D. H. Lee, J. Y. Kim, T. H. Han, B. H. Kim, M. Park, K. No, and S. O. Kim, J. Mater. Chem., **21**, 3432-3437 (2011).

Chapter 2

Highly transparent and flexible field electron emitter based on single-walled carbon nanotube

2.1 Introduction

Transparent electronics has been applied in numerous fields such as transistors, solar cells and light-emitting devices due to its great potential to make significant impact in a wide variety of areas [1-3]. So far, various kinds of transparent and flexible display devices have been studied [4-6]. FEDs are such kind of display which fits in this category [7-9]. To realize this display, it requires suitable materials which can grow on plastic substrate by low temperature fabrication process [10-13].

Recently, flexible FE properties have been studied of CNF grown on plastic substrate by ion-beam method [14]. Watts et al. reported the polymer supported CNTs array to develop flexible FED [15]. Recently, transparent FE devices have been developed based on SWCNTs and spin on glass (SOG) composite materials [16].

Recently, my groups have been developed the transparent and flexible FEDs by the formation of CNCSs on nafion substrate [17]. However, the non-conductivity and the low FE property of the CNCSs were the two major issues inhibiting the large scale fabrication of this device. Materials like carbon nanostructures, ZnO based nanostructures and graphene based structures have been studied for the development of FEDs [18-20]. Among them, CNTs are very effective for FEDs due to their sharp emission tips, high aspect ratio and good environmental stability etc. [21-23].

With this motivation, in this Chapter we report the fabrication of SWCNTs based

FEE and their application towards transparent and flexible FEDs has been studied. The fabrication of SWCNTs as FEEs is an important advance for the fabrication of next generation transparent and flexible FEDs.

2.2 Experiment

2.2.1 Purification of SWCNTs

Purification of CNTs are the initial step to get good quality film, as the unwanted materials like amorphous carbon, metal particles severely affect CNTs' properties [24]. Several purification methods have been described to purify the CNTs like oxidation, purification by strong acid, annealing and functionalization of CNTs etc. [25-28]. In the present case for the purification of CNTs, I annealed the CNTs in the temperature range 400 to 450 ^{0}C. In this temperature region, the amorphous carbon are removed and the metal catalyst particles are melted and as a result of it the graphitic properties of CNTs are also improved.

2.2.2 Fabrication of SWCNTs film on arylite substrate

Here I used a spray coating method for thin film formation of SWCNTs dispersed in DCE solution. DCE is proved to be an effective solvent for SWCNTS dispersion.

Since DCE is very volatile and suitable for suspending SWCNTs in wetting any substrate, I was successfully able to make a uniform film. As received laser ablated

SWCNTs were used as a starting material. At first, desired amount of SWCNTs was added to DCE to a make highly dispersed SWCNTs solution. The solution was ultrasonicated for about 4 h followed by centrifugation at a speed of 10000 rpm for 30 minutes to separate out undissolved heavier SWCNTs bundles and impurities. After centrifugation, the suspension was decanted so that only the supernatant of the centrifuged material was incorporated in the final suspension. SWCNTs films were made by spray coating of SWCNTs dispersed in DCE onto an extremely heat tolerant arylite substrate (1.5 cm ×1.5 cm) (glass transition temperature = 330 ^{0}C).

2.2.3 Field emission measurement

Field electron emission characteristics of the SWCNTs film on the arylite substrate were measured at a typical working pressure of 3.0×10^{-4} Pa in an O-ring-shield glass chamber evacuated continuously by a turbo molecular pump. The cathode was separated by 100 μm from the SWCNTs based anode by a transparent and flexible arylite spacer. The emission area was 0.1 cm^2.

2.3 Results and discussion

2.3.1 Morphology and the characterization of the SWCNTs film

The morphology of the SWCNTs film was carefully examined by field emission scanning electron microscopy (FESEM, HITACHI S-4300, and Scanning Electron

Microscope) and atomic force microscopy (AFM, JEOL JSPM-5200 TM, Scanning Probe Microscope).

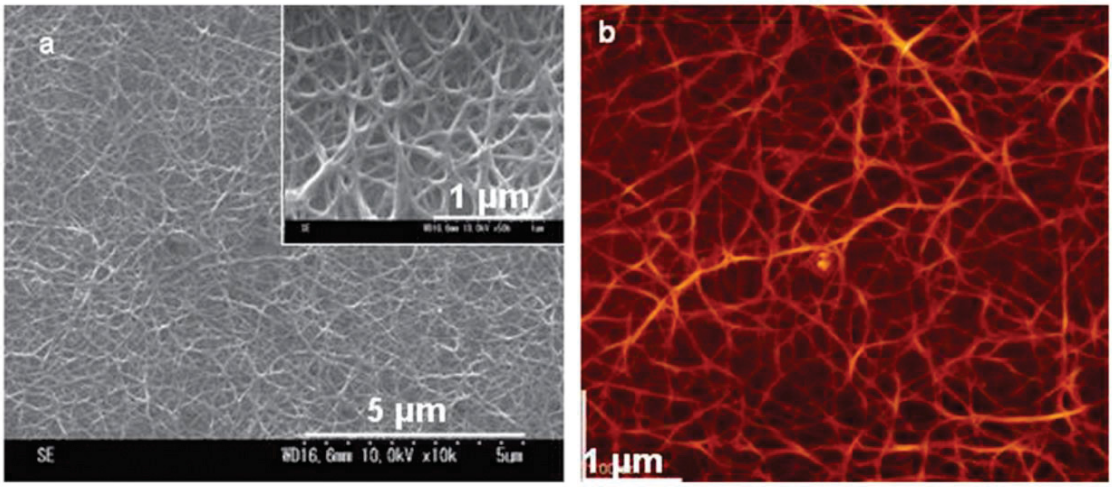

Fig. 2.1 (a) FESEM image of SWCNTs film on arylite substrate (b) a typical AFM image of SWCNTs/arylite film.

A FESEM image of the SWCNTs film on the arylite substrate is shown in Fig. 2.1a. The inset of Fig. 2.1a depicts the magnified image of the SWCNTs film. Observation of the FESEM image indicates that the surface was fully covered with nanotubes network. The network of SWCNTs in this picture has a clean surface. Fig. 2.1b shows the AFM image of the SWCNTs film. AFM clearly reveals that the SWCNTs network distributed homogeneously on to the arylite substrate.

2.3.2 Raman study of the SWCNTs film

Fig. 2.2 shows the Raman spectrum of the SWCNT sample. The Raman spectrum (JASCO, NRS-1500W) was measured with an excitation wavelength of 532 nm from a

green laser with a typical acquisition time of 300 s. The presence of a radial breathing mode (RBM) peak near at 172 cm^{-1} , and the quite low intensity ratio of the defect-induced D-band at 1352 cm^{-1} and the tangential G-band near at 1596 cm^{-1} (I_D/I_G = ~0.06) are indicative the presence of high quality SWCNTs.

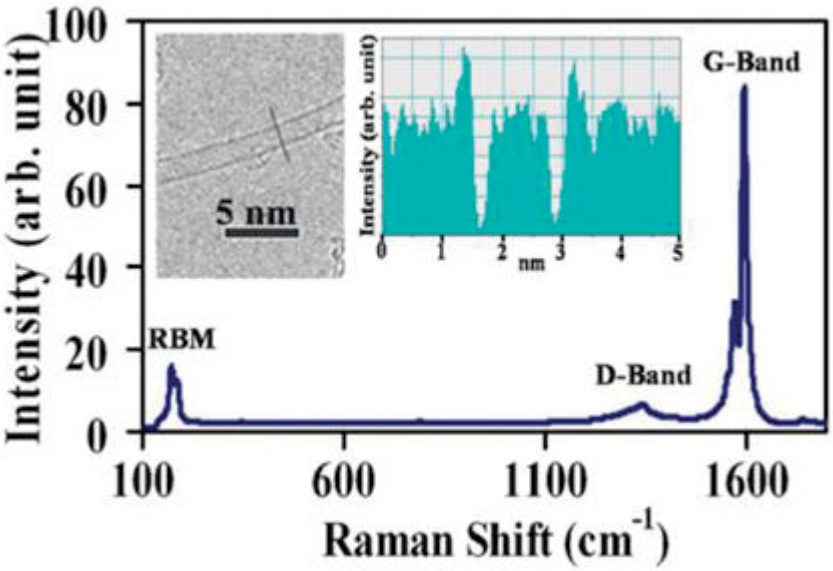

Fig. 2.2 The Raman spectrum of SWCNTs and inset show the intensity profile of an isolated SWCNTs along the marked line.

The diameter of SWCNTs was calculated from the RBM peak frequency (ω in cm^{-1}) using the relation d [nm] = 248/ω [29]. According to the above expression, the RBM frequency of 172 cm^{-1} corresponds to the SWCNTs with the diameter of 1.44 nm. This result is consistent with the high resolution transmission electron microscopy image

(HRTEM, JEOL, JEM2100F) shown in the inset of the Fig. 2.2 with an intensity profile along the marked line placed at the right hand side.

2.3.3 Study of the UV-Vis spectra

Fig. 2.3 shows the UV-Vis spectroscopy of the SWCNTs film with an optical range of wavelength measured using a spectrophotometer (Shimadzu, UV-1800). At 550 nm, the transmittance of the film was found to be 86%.

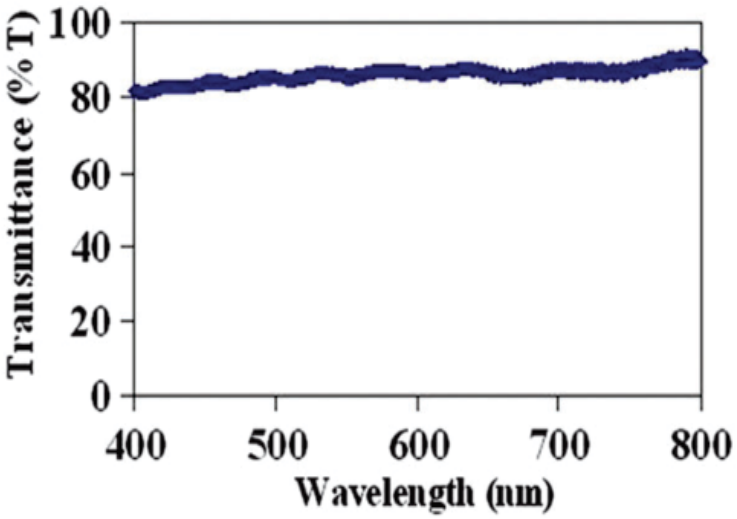

Fig. 2.3 UV-Vis spectrum of SWCNTs film fabricated on arylite substrate.

The sheet resistance of the film was measured using four probes measurement. The sheet resistance of the SWCNTs film was found to be 1.7 kΩ/sq. The sheet resistance value is lower than the previously reported HIPCO grown SWCNTs [30-31]. The conductivity of the film could be improved by increasing the thickness. However, with increasing the thickness, the transparency of the film was decreased. Thus from an

application point of view a balancing between transparency and conductivity is highly required. Thus to maintain the high transparency of the emitters, the film thickness was well optimized to obtain superior field electron emission performance of the film.

2.3.4 FE Study

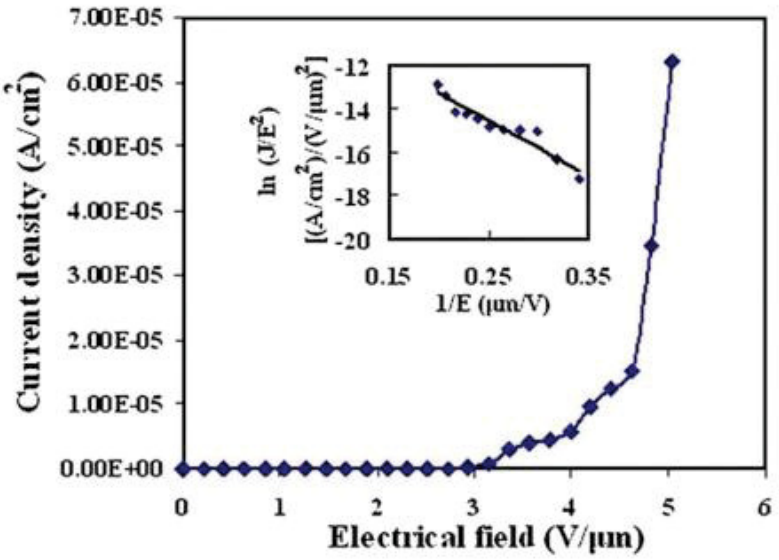

Fig. 2.4 FE property of SWCNTs/arylite film and inset shows the Fowler-Nordheim (F-N) plot.

The field electron emission characteristic of the film is shown in Fig. 2.4. The turn-on field corresponding to the current density of 0.1 mA cm^{-2} was 2.8 V μm^{-1}. Similarly, the threshold field, defined as the field required to extract current density of 10 $mAcm^{-2}$, was observed to be 4.2 V μm^{-1}. A recent study showed that CNCSs fabricated on a transparent and flexible nafion substrate are effective electron emitters. For CNCSs based emitters, the turn-on and threshold fields were observed to be 6.1 V μm^{-1} (for 10

nA cm^{-2}) and 9.5 V μm^{-1} (10 μA cm^{-2}), respectively. For SWCNTs based emitters, both turn-on and threshold fields are much lower than the CNCSs based transparent and flexible FEE [17]. The better FE performance of the present SWCNTs film is likely to be caused by lower dimension of the SWCNTs compared to the CNCSs and by higher conductivity of the SWCNTs film than the CNCSs based emitter. Thus the concept of SWCNTs/arylite based flexible emitter may open up opportunities in future highly transparent and flexible displays that are portable, light weight and can be fabricated to the desired shape for better viewing angles and of high resolution.

The inset of Fig. 2.4 shows the F–N plot. The straight line indicates that emission behavior follows the F–N model and it can be defined as cold electron FE. The value of β was found to be 3066. The β was much higher than the CNCSs based emitters, indicating that SWCNTs based films are promising candidates for the FE source and development of future transparent and rollable FEDs.

The photograph shown in Fig. 2.5a depicts the flexibility of the SWCNTs film. Fig. 2.5b illustrates the photograph of the whole device. It was observed from Fig. 2.5b that the image placed under the cathode, anode and spacer was clearly visible. This means that my FED was highly transparent. To demonstrate the light emitted image, at the preliminary stage, an unbendable calcium fluoride (CaF_2) phosphor has been used.

Fig. 2.5 (a) A SWCNTs based flexed arylite film (b) Transparent FE device consisting of the SWCNTs/arylite film as both cathode and anode together with an arylite spacer (insulator) on a printed picture, confirming the transparency of the whole device. (c) Blue light image using CaF_2 as a phosphor screen.

A very thin layer of gold was coated onto CaF_2. Fig. 2.5c shows the highly bright blue light image captured during the FE experiment.

2.4 Conclusion

I demonstrated the successful fabrication of SWCNTs based highly transparent (transparency = 86%) and flexible FEE with turn-on and threshold fields of 2.8 and 4.2 V μm^{-1}, respectively. My experimental result reveals that the SWCNTs based film is overwhelmingly better than the previously reported CNCSs based film in all of the vital aspects, including transparency, conductivity and FE performance. Still there are some leftover issues such as fabrication of transparent, flexible and conductive phosphor materials which are the main obstacles for the fabrication of entire transparent and flexible device. The work related to this issue is currently going on. SWCNTs based transparent, flexible and conductive films have considerable potential for next generation transparent and flexible FEDs due to their simplicity of fabrication, portability, low production costs, scale-up for a large sized display etc. Transparent and flexible FEDs could open up exciting device application for so-called head-up displays and highly intelligent

information displays as a useful step, advancing towards the ubiquitous society.

2.5 References

[1] John. F. Wager, Science, **300**, 1245-1246 (2003).

[2] C.-C Chen, L. Dou, R. Zhu, C.-H. Chung, T.-B. Song, Y. B. Zheng, S. Hawks, G. Li, P. S.Weiss, and Y. Yang, ACS Nano **6**, 7185-7190 (2012).

[3] M.-S. Lee, K. Lee, S.-Y. Kim, H. Lee, J. Park, K.-H. Choi, H.-K. Kim, D.-G. Kim, D.-Y. Lee, S. W. Nam, and J.-U. Park, Nano Lett., **13**, 2814-2821 (2013).

[4] P. Görrn, M. Sander, J. Meyer, M. Kröger, E. Becker, H.-H. Johannes, W. Kowalsky, and T. Riedl, Adv. Mater., **18**, 738-741 (2006).

[5] C. Jang, K. Kim, and K. C. Choi, IEEE Electron Device Lett., **33**, 74-76 (2012).

[6] C. Schrage and S. Kaskel, ACS Appl. Mater. Interfaces, **1**, 1640-1644 (2009).

[7] X. Guo and S. R. P. Silva, IEEE Electron Device Lett., **28**, 710-712 (2007).

[8] A. A. Kuznetzov, S. B. Lee, M. Zhang, R. H. Baughman, A. A. Zakhidov, Carbon, **48,** 41-46 (2010).

[9] A. A. G. D.-Smith, D. G. Hasko, and H. Ahmed, Appl. Phys. Lett. **71**, 3159-3161 (1997).

[10] S. Hofmann, C. Ducati, B. Kleinsorge, and J. Robertson, Appl. Phys. Lett. **83**, 4661-4663 (2003).

[11] H. S. Sim, S. P. Lau, H. Y. Yang, and L. K. Ang, M. Tanemura and K. Yamaguchi,

Appl. Phys. Lett. **90**, 143103-3 (2007).

[12] H. Y. Yang, S. P. Lau, S. F. Yu, L. Huang, M. Tanemura, J. Tanaka, T. Okita, and H. H. Hng, Nanotechnology, **16**, 1300-1303 (2005).

[13] L.Yuan, Y. Tao, J. Chen, J. Dai, T. Song, M. Ruan, Z. Ma, L. Gong, K. Liu, X. Zhang, X. Hu, J. Zhou, and Z. L. Wang, Adv. Funct. Mater. **21**, 2150-2154 (2011).

[14] T. T. Tan and H. S. Sim, S. P. Lau, H. Y. Yang, M. Tanemura and J. Tanaka, Appl. Phys. Lett. **88**, 103105-3 (2006).

[15] P. C. P. Watts, S. M. Lyth, E. Mendoza, and S. R. P. Silva, Appl. Phys. Lett. **89**, 103113-3 (2006).

[16] N. V. Quy, N. D. Hoa, Y. Cho, D. Oh, H. Song, Y. Kang, D. Kim, J. Cryst. Growth **311**, 662-665 (2009).

[17] P. Ghosh, M. Z. Yusop, S. Satoh, M. Subramanian, A. Hayashi, Y. Hayashi, and M. Tanemura, J. Am. Chem. Soc. **132**, 4034-4035 (2010).

[18] G Pirio, P. Legagneux, D. Pribat, K. B. K. Teo, M. Chhowalla, G. A. J. Amaratunga, and W. I. Milne, Nanotechnology **13**, 1-4 (2002).

[19] Ke. Yu, Y. S. Zhang, F. Xu, Q. Li, Z. Q. Zhu, and Q. Wan, Appl. Phys. Lett. **88**, 153123-3 (2006).

[20] Z.-S. Wu, S. Pei, W. Ren, D. Tang, L. Gao, B. Liu, F. Li, C. Liu, and H.-M. Cheng,

Adv. Mater. **21**, 1756-1760 (2009).

[21] R. C. Smith, D. C. Cox, and S. R. P. Silva, Appl. Phys. Lett. **87**, 103112-3 (2005).

[22] J. Y. Huang, K. Kempa, S. H. Jo, S. Chen, and Z. F. Renb, Appl. Phys. Lett. **87**, 053110-3 (2005).

[23] A. S. Barnard, Phys. Chem. Chem. Phys., **14**, 10080-10093 (2012).

[24] Y. F. Hu, X. L. Liang, Q. Chen, and L.-M. Peng, Z. D. Hu, Appl. Phys. Lett. **88**, 063113-3 (2006).

[25] P.-X. Hou, C. Liu, H.-M. Cheng, Carbon, **46**, 2003-2025 (2008).

[26] H. Hu, B. Zhao, M. E. Itkis, and R. C. Haddon, J. Phys. Chem. B, **107**, 13838-13842 (2003).

[27] H. Zhang, C. H. Sun, F. Li, H. X. Li, and H. M. Cheng, J. Phys. Chem. B, **110**, 9477-9481 (2006).

[28] V. Georgakilas, D. Voulgaris, E. Vazquez, M. Prato, D. M. Guldi, A. Kukovecz, and H. Kuzmany, J. am. Chem. Soc. **124**, 14318-14319 (2002).

[29] R. Saito, G. Dresselhaus and M. S. Dresselhaus, Phys. Rev. B: Condens. Matter, **61**, 2981-2990 (2000).

[30] D. Zhang, K. Ryu, X. Liu, E. Polikarpov, J. Ly, M. E. Tompson and C. Zhou, Nano Lett., **6**, 1880-1886 (2006).

[31] E. Artukovic,M. Kaempgen, D. S. Hecht, S. Roth and G. Grulner, Nano Lett., **5**, 757-760 (2005).

Chapter 3

Fabrication of transparent and flexible anode and its application in FEDs

3.1 Introduction

Recently, FEDs have attracted much attention as it considered for the fabrication of future FPDs. These displays can be applied in various fields such as windshields, computer and other electronic devices etc. There are two main components for FEDs: a cathode material which emits the electron and the anode material at which the emitted electrons are drained out through the phosphor material.

The most commonly used anode material in FEDs is ITO due to its good optoelectronic properties [1-3]. However, owing to the stiffed nature of the anode material, it inhibits the manufacture of whole device transparent and flexible. Thus the fabrication of suitable phosphor materials onto the transparent and flexible substrate is a preliminary step to realize the whole device transparent and flexible. These phosphor materials possess the following characteristic features like high efficiency, good luminescence properties and low voltage electron excitation etc.

Much effort has been devoted for the fabrication of the phosphor materials to develop the FEDs [4-6]. However, in most of the cases the fabrication of phosphor materials has grown on stiff and opaque substrates [7-9]. Recently, Jang et al. has been developed the polyvinyl alcohol-slurry screen technology of phosphor material and applied in FEDs [10].

Until now, few methods have been developed to fabricate the transparent and flexible FEDs based on carbon nanomaterials [11-12]. Arif et al. has been developed the transparent and flexible FEDs based on metallic nanowire and graphene [13]. In my previous studies, I have successfully fabricated transparent and flexible FEDs based on SWCNTs films as cathode and ITO coated glass as anode material. For light emission image, I used Au coated CaF_2 as screen. Thus the fabrication of the phosphor material

onto the transparent and flexible substrate is the key to realize the whole device transparent and flexible.

In an effort to produce a transparent and flexible phosphor screen on conductive substrate, the direct fabrication of metavanadate phosphors AVO_3 (A = K, Rb and Cs) at room temperature has been developed by Nakajima et al. [15]. They investigated the luminescent color and quantum efficiency of these broad-band-emitting metavanadate phosphors, and results indicate that they have huge potential for lighting applications. The direct fabrication of phosphor oxide films at low temperature was highly advantageous due to the simple fabrication technique and the low cost of fabrication on transparent and flexible substrate compared to the conventional high-temperature growth process of making phosphor [16-18]. The successful fabrication of transparent and flexible phosphor on conductive plastic substrate has paved the way for fabricating the entire device transparent and flexible.

In this Chapter, I fabricated highly transparent and flexible FEDs consisting of SWCNTs/arylite film as FEE and a metavanadate phosphor on an SWCNT-based transparent, flexible and conductive film as screen. SWCNTs are considered to be an ideal candidate for next-generation FEDs due to their extraordinary physical properties and superior FE performance [19-22]. The as-prepared SWCNTs/arylite film showed good transparency and superior FE performance with appreciable amount of emission current

density. The fabrication of the SWCNT-based transparent and flexible film has already been reported in my earlier work [13].

3.2 Experimental details

The fabrication of SWCNTs film on arylite substrate was described in Chapter 2. Here I used commercially available arc discharge grown SWCNTs instead of laser ablated SWCNTs.

For preparing the screen, $CsVO_3$ was used as green phosphor and coated on to SWCNT-based transparent, flexible and conductive arylite substrate at room temperature. The procedure for the synthesis of $CsVO_3$ has been discussed elsewhere in detail [15]. A flow diagram is shown in Fig. 3.1 demonstrating the fabrication of cathode and the anode material.

3.2.1 Fabrication of cathode and anode

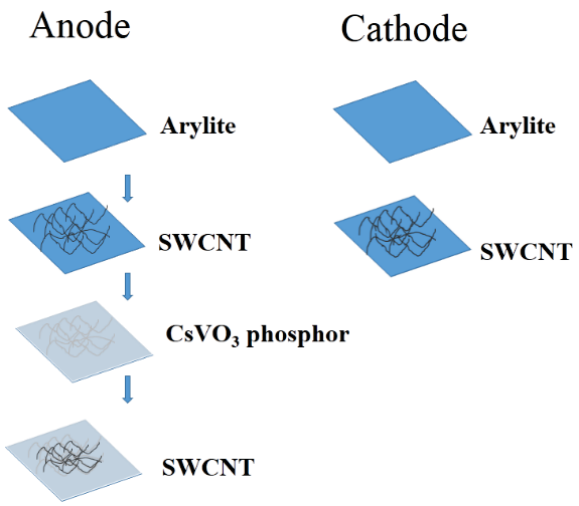

Fig. 3.1 A schematic scheme for the fabrication of cathode and the screen (anode).

3.3 Results and discussion

3.3.1 Morphological Study of the Film

The SEM and AFM images show that bundles of SWCNTs were randomly distributed and interconnected forming a dense and homogeneous film shown in Fig. 3.2a and 3.2b, respectively.

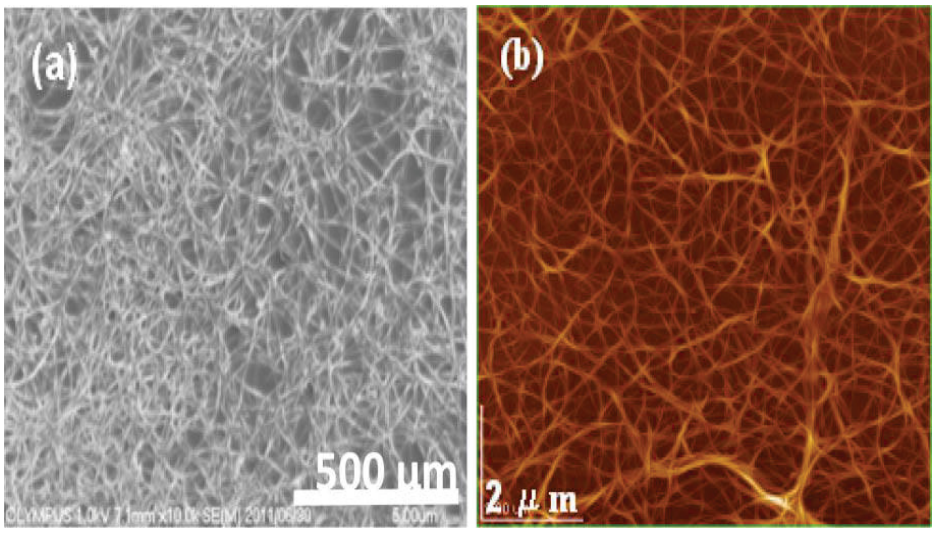

Fig. 3.2 (a) A Typical SEM and (b) AFM image of SWCNTs film fabricated on arylite substrate.

The intensity profile along the small horizontal line in Fig. 3.3a is shown in Fig. 3.3b. From the TEM intensity profile, the diameter of an isolated SWCNT was determined to be 1.75 nm.

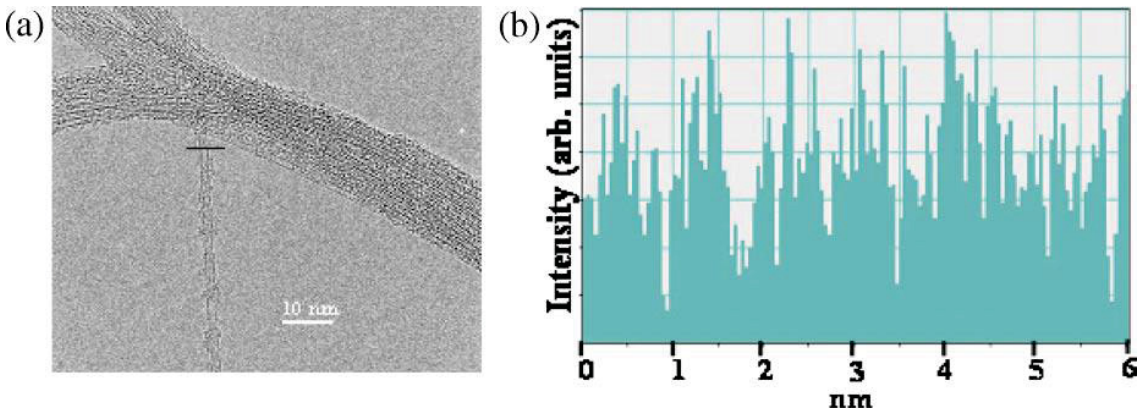

Fig. 3.3 (a) Typical HRTEM image and (b) the intensity profile of an individual SWCNTs along the horizontal line.

The transmittance of the films were measured by UV–Vis spectrophotometer and the results are shown in Fig. 3.4. The transmittance of the SWCNT film was observed to be 92.6% at 550 nm. The transmittance of the screen decreased dramatically after depositing green phosphor onto it and was found to be 54%.

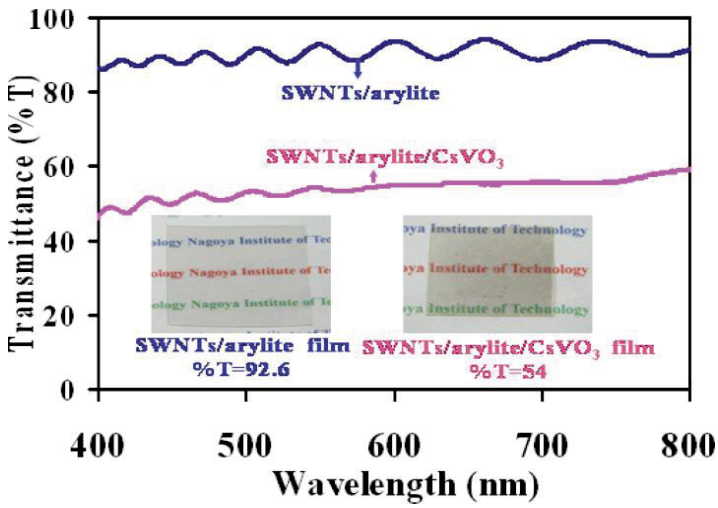

Fig. 3.4 UV–Vis spectra of SWCNTs/arylite (blue line) and SWCNTs/arylite/$CsVO_3$ film (pink line). A sheet of paper with letters was placed underneath the SWCNTs/arylite (left side) and SWCNTs/arylite/$CsVO_3$ (right side) film to check the transparency of the films.

However, there is still need to improve the transparency of the phosphor. Better control of the thickness of both the SWCNT and phosphor film seems to be necessary for further transmittance improvement. I am currently trying to optimize these properties. The insets of Fig. 3.4 depict the transparent nature of the flexed films. A sheet of lettered paper placed underneath the flexed SWCNT-based emitter and screen was clearly visible, indicating the transparency of the film. The varying clearness of the letters is attributed to the phosphor coating on the SWCNTs/arylite film. The sheet resistance of the SWCNTs/arylite film was measured using four-probe measurement. The optimized film shows a sheet resistance of 23 kΩ/sq at 92.6% transparency. It is pertinent to mention that the sheet resistance value was strongly influenced by the thickness of the film (not shown here) and it could be enhanced by increasing the thickness of the film. However, higher thickness of the SWCNT film will reduce the transparency of the substrate. So the film of lower thickness was maintained to obtain high optical transparency of the film for the demonstration of transparent and flexible FEDs.

3.4 FE study

3.4.1 FE device diagram

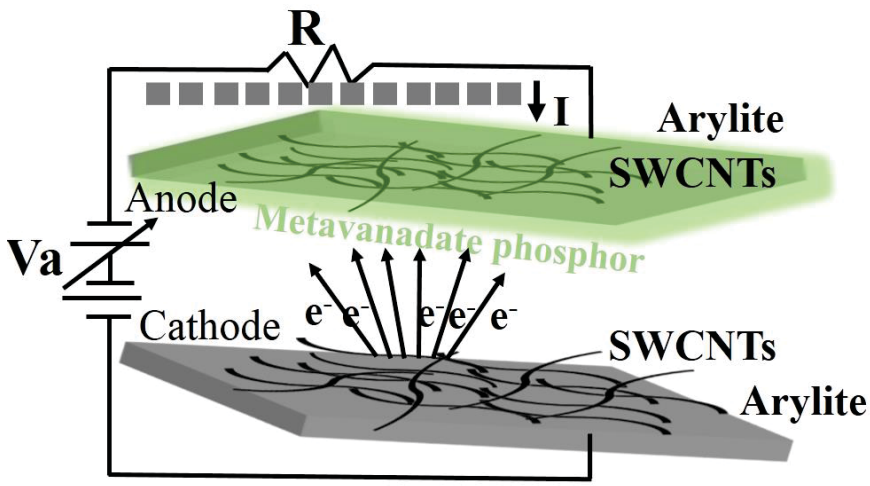

Fig. 3.5 A schematic diagram for FE device, SWCNTs coated on arylite film was used as cathode and SWCNTs/arylite/$CsVO_3$ used as a screen.

A schematic diagram of SWCNT based FE device is shown in Fig. 3.5. SWCNTs coated on arylite substrate was used as a cathode and metavanadate phosphor coated on SWCNTs network was the anode material.

3.4.2 FE results

Figure 3.6 shows the plot of electrical field (E) vs. current density (J). The turn-on field corresponding to the current density of 10 μA/cm^2 was 5.6 V/μm whereas the threshold field corresponding to the current density of 100 μA/cm^2 was 8.8 V/μm.

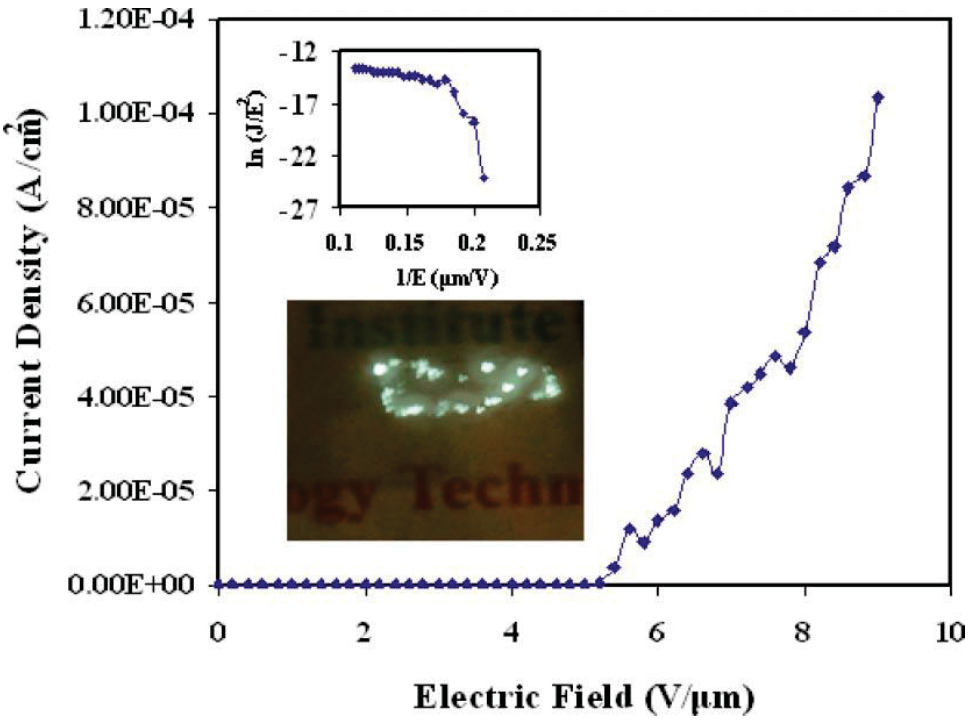

Fig. 3.6 FE curve of SWCNTs/arylite film using SWCNTs/arylite/$CsVO_3$ used as a screen. Top inset: F–N plot. Bottom inset: Transparency of the whole device; the letters placed under cathode, spacer and screen were noticeably visible during observing a green-light image.

Lahiri et al. reported the fabrication of graphene-based flexible and transparent FEDs, composed of multiwall CNTs (MWCNTs) over graphene as cathode and phosphor-coated graphene as anode [23]. In their proposed design of the device, graphene film on plastic substrate acts as the conductive substrate while MWCNTs coated on top of it perform as electron emitters. The hybrid CNT–graphene structure was used for the fabrication of transparent and flexible FEE. In order to simplify this structure, an SWCNT-based film could be a suitable substitute of the hybrid CNT–graphene structure due to the extraordinary physical properties of SWCNTs: They have a huge potential in

FEDs owing to their high aspect ratio, low work function, and chemical inertness etc. and showed their importance as highly transparent and flexible FEE. Lahiri et al. also mentioned the fabrication of a transparent and flexible screen by dip coating of graphene/ PET substrate into green phosphor–water solution [23]. This indirect procedure is quite time-consuming. Again there was no data provided about the transmittance of the phosphor screen. In this regard my metavanadate phosphor on SWCNTs/arylite film is thought to be a better candidate due to its direct fabrication on the transparent, flexible and conductive SWCNTs/arylite film at room temperature. Although the FE performance is lower than that of the MWCNT–graphene based hybrid structures, from the transparency point of view, the current device is better than the MWCNT–graphene based transparent and flexible FEDs [23]. The top inset of Fig. 3.6 shows the F–N plot. A straight line in this plot signifies that the emission behavior follows the F–N model. This simply implies that SWCNTs could be suitable emitters for the fabrication of future transparent and flexible FEDs. The bottom inset of Fig. 3.6 shows the transparency of the whole device during observing a green light image, it was found that the letters placed under the cathode, spacer and phosphor screen were visible. However, the lower clarity of the letters was due to low light environment inside the emission chamber. The non-uniform emission might originate from the screening effect of the neighboring nanotubes

due to their high density and low thickness (height). Overall, the SWCNT-based emitters on arylite substrate and metavanadate-based phosphor on SWCNT/arylite substrate have a huge potential for future transparent and flexible FEDs.

3.5 Conclusion

An entire SWCNT-based transparent and flexible FED has been developed by fabricating highly transparent FEE and screen. An extremely simple spray coating method has been used to fabricate transparent and flexible electron emitters. A novel $CsVO_3$ is considered to be a promising phosphor and was fabricated directly on SWCNT/arylite-based conductive, flexible and highly transparent substrate. SWCNT-based emitters and screen exhibit optical transmission of 92.6% and 54%, respectively. FE measurements indicated that SWCNT-based films are quite effective emitters and produce significant amount of current density. There is still need for improvement of the transmittance of the phosphor; I am presently working to resolve this matter.

3.6 References

[1] I. Musa, D. A. I. Munindrasdasa, G. A. J. Amaratunga and W. Eccleston, Nature **395**, 362-365 (1998).

[2] C. J. Lee, T. J. Lee, S. C. Lyu, and Y. Zhang, H. Ruh and H. J. Lee, Appl. Phys. Lett. **19**, 3648-3650 (2002).

[3] Y.-M. Chang, P.-H. Kao, H.-M. Tai, H.-W. Wang, C.-M. Lin, H.-Y. Leede, and J.-Y. Juang, Phys. Chem. Chem. Phys. **15**, 10761-10766 (2013).

[4] X. Liu, and J. Lin, Appl. Phys. Lett. **90**, 184108-3 (2007).

[5] P. H. Holloway, T. A. Trottier, J. Sebastian, S. Jones, X.-M. Zhang, J.-S. Bang, B. Abrams, W. J. Thomes, and T.-J. Kim, J. Appl. Phys. **88**, 483-488 (2000).

[6] M. Shang, G. Li, D. Yang, X. Kang, C. Peng, Z. Cheng, and J. Lin, Dalton Trans. **40**, 9379-9387 (2011).

[7] C. Zhang and J. Lin, Chem. Soc. Rev. **41**, 7938-7961 (2012).

[8] D. Geng, G. Li, M. Shang, C. Peng, Y. Zhang, Z. Cheng, and J. Lin, Dalton Trans. **41**, 3078-3086 (2012).

[9] H. Nersisyan, H. I. Won, and C. W. Won, Chem. Commun. **47**, 11897-11899 (2011).

[10] J. E. Jang, J.-H. Gwak, Y. W. Jin, S. J. Lee, S. H. Park, J. E. Jung, N. S. Lee, and J. M. Kim, J. Vac. Sci. Technol. B, **18**, 1106-1110 (2000).

[11] P. Ghosh, M. Z. Yusop, S. Satoh, M. Subramanian, A. Hayashi, Y. Hayashi, and M. Tanemura, J. Am. Chem. Soc. **132**, 4034-4035 (2010).

[12] A. A. Kuznetzov, S. B. Lee, M. Zhang, R. H. Baughman, A. A. Zakhidov, Carbon **48**, 41-46 (2 0 1 0).

[13] M. Arif, K. Heo, B. Y. Lee, J. Lee, D. H. Seo, S. Seo, J. Jian, and S. Hong, Nanotechnology **22**, 355709-7 (2011).

[14] D. Ghosh, P. Ghosh, M. Tanemura, A. Haysahi, Y. Hayashi, K. Shinji, N. Miura, M. Z. Yusop, and T. Asaka, Chem. Commun. **47**, 4980-4982 (2011).

[15] T. Nakajima, M. Isobe, T. Tsuchiya, Y. Ueda, and T. Kumagai, Nature Mater. **7**, 735-740 (2008).

[16] K.-B. Kim, Y.-I. Kim, H.-G. Chun, T.-Y. Cho, J.-S. Jung, and J.-G. Kang, Chem. Mater. **14**, 5045-5052 (2002)

[17] T. Kyomen, R. Sakamoto, N. Sakamoto, S. Kunugi, and M. Itoh, Chem. Mater. **17**, 3200-3204 (2005).

[18] C.-C. Kang, R.-S. Liu, J.-C. Chang, and B.-J. Lee, Chem. Mater. **15**, 3966-3968 (2003).

[19] E. Stratakis, E. Kymakis, E. Spanakis, P. Tzanetakis, and E. Koudoumas, Phys. Chem. Chem. Phys. **11**, 703-709 (2009).

[20] C. J. Shearer, J. Yu, K. M. O'Donnell, L. Thomsen, P. C. Dastoor, J. S. Quinton, and J. G. Shapter, J. Mater. Chem. **18**, 5753-5760 (2008).

[21] W. I. Milne, K. B. K. Teo, G. A. J. Amaratunga, P. Legagneux, L. Gangloff, J.-P. Schnell, V. Semet, V. Thien Binh, and O. Groening, J. Mater. Chem. **14**, 933-943 (2004).

[22] N. Liu, G. Fang, W. Zeng, H. Zhou, H. Long and X. Zhao, J. Mater. Chem., **22**, 3478-3484 (2012).

[23] I. Lahiri, V. P. Verma, W. Choi, Carbon. **49**, 1614-1619 (2011).

Chapter 4

Modification of conducting polymer surface for efficient transparent and flexible field electron emitter

4.1 Introduction

Compared with rigid or transparent FEDs, transparent and flexible FEDs have attracted much attention in recent years [1-3]. Transparent and flexible FED have been applied for future portable and rollable displays [4]. To develop this display, a proper selection of suitable FEE is essential, which has high transparency with good flexibility and reliable emission properties. However, CNTs based FEE shows good emission properties with reasonable transparency [5]. To increase the FE device performance, researchers have been developed hybrid structures, decoration of nanoparticles on SWCNTs surface, and ion beam irradiation on CNTs film etc. [6-8]. The hybrid structures show better properties than their individual component [9].

Recently, Lahiri et al. have been reported the emission properties of the hybrid structure of graphene with CNTs [10]. The fabrication of graphene on copper substrate requires a high growth temperature and their transfer onto a flexible substrate is an extremely strenuous task. In this method the hybrid structure of graphene with CNTs showed good FE properties but their transparency was the major obstacle to fabricate the large scale applications. Hwang et al. studied the emission behavior of vertically aligned ZnO nanowire grown on reduced graphene/polydimethylsiloxane (PDMS) substrate [11]. This hybrid material shows low transparency and the reduction of the graphene oxide is high

growth temperature process. In this regard, the hybrid structure of PEDOT:PSS with CNTs might be helpful to fabricate the efficient FEE.

PEDOT:PSS is a quite promising material towards next-generation smart devices due to its high conductivity with good transparency, water solubility and good environmental stability etc. [12-15]. Besides this, PEDOT:PSS material can be easily fabricated on large-area plastic substrate by simple spin coating [16]. A combined structure of conducting polymer (PEDOT:PSS) and SWCNTs might be a supreme architecture for the fabrication of transparent and flexible FEE as both of these candidates have interesting properties. SWCNTs serve as an effective emitter whereas PEDOT:PSS makes the substrate very much conductive. I took the advantage of these two materials and fabricated highly transparent and flexible FEE. In the work described in this Chapter, I fabricated hybrid thin films based on SWCNTs/PEDOT:PSS on PET substrate for the fabrication of transparent and flexible FEDs.

4.2 Experiment

4.2.1 Fabrication of the PEDOT:PSS film on PET

The conducting polymer PEDOT:PSS was purchased from Polysciences, Inc. One drop of PEDOT:PSS (1 wt%) solution was added to 20 ml water. This diluted solution of PEDOT:PSS was drop casted on PET substrate which was placed on a heater

at 150 °C. After the evaporation of water, the PEDOT:PSS based PET substrate was immersed in an ethylene glycol bath for 3 min. Finally, the ethylene glycol treated PEDOT:PSS film was annealed at 150 °C for 20 min.

4.2.2 Fabrication of the PEDOT:PSS/SWCNTs film

The purification, dispersion of SWCNTs in organic solvent and the fabrication of thin film onto plastic substrate was described in the Chapter 2. The conductivity of the hybrid PEDOT:PSS/SWCNTs film is decreased due to the chemical reaction between PEDOT:PSS and DCE. The detailed mechanism of decreased the conductivity of the hybrid film is unknown. To avoid the chemical reaction on PEDOT:PSS surface by DCE, I used here ethanol to disperse the SWCNTs. 1 ml ethanol dispersed SWCNTs (conc. 1 mg/40 ml) solution was spray coated on bare PET and PEDOT:PSS-based PET surfaces to prepare two different kinds of thin film. The distance between the sample and the nozzle of the spray coater was 20 cm and the gas pressure was fixed at 0.05 MPa.

4.3 Results and discussions

4.3.1. Morphology of SWCNTs and PEDOT:PSS/SWCNTs film

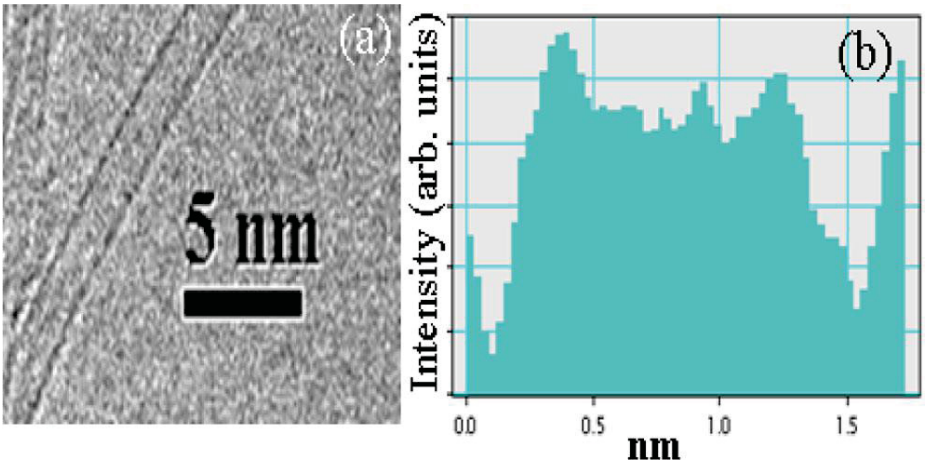

Fig. 4.1 (a) HRTEM image of an individual SWCNT (b) intensity profile of an isolated SWCNT.

A typical HRTEM was used to evaluate the presence of SWCNTs, as shown in Fig. 4.1. The diameter of the individual SWCNTs was observed to be around 1.5 nm. The intensity profile of SWCNTs is shown in Fig. 4.1b. The PEDOT:PSS and PEDOT:PSS/SWCNTs thin films were characterized by AFM as shown in Fig. 4.2.

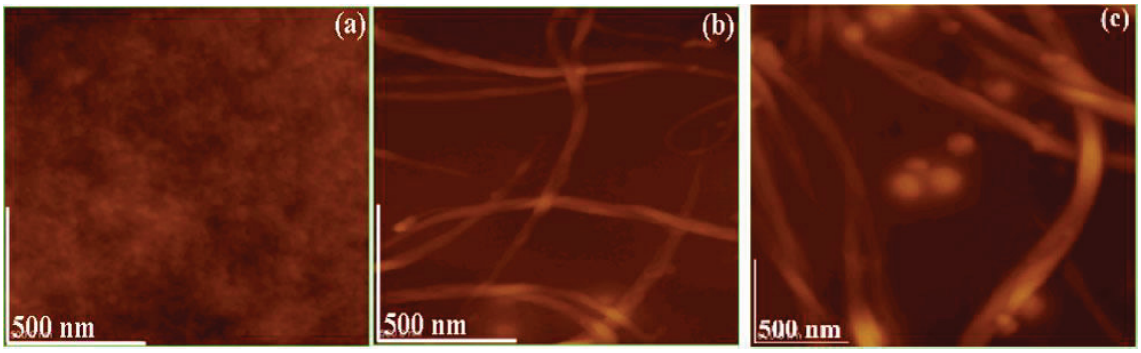

Fig. 4.2 Typical AFM images of (a) PEDOT:PSS film, (b) PEDOT:PSS/SWCNTs film, and (c) SWCNTs film on PET substrate

From Fig. 4.2a it is seen that the surface of the PEDOT:PSS film was uniform,

which was due to the well dispersed PEDOT:PSS solution in water. From Fig. 4.2b and 4.2c it was confirmed that the SWCNTs were nicely distributed on the PEDOT:PSS surface.

Figure 4.3 shows the UV–Vis spectra of PEDOT:PSS/SWCNTs film on PET substrate. At 550 nm, the transparency of PEDOT:PSS/SWCNTs film was observed as 93%. The UV–Vis data showed that my hybrid film was highly transparent. The sheet resistance of the PEDOT:PSS film was measured using four-probe measurement (NAPSON CORPORATION, RG-7c, model RT-7oV) and was found to be 3.5 kΩ/sq. The PEDOT:PSS-based PET film was immersed in ethylene glycol bath for 3 min to enhance the conductivity.

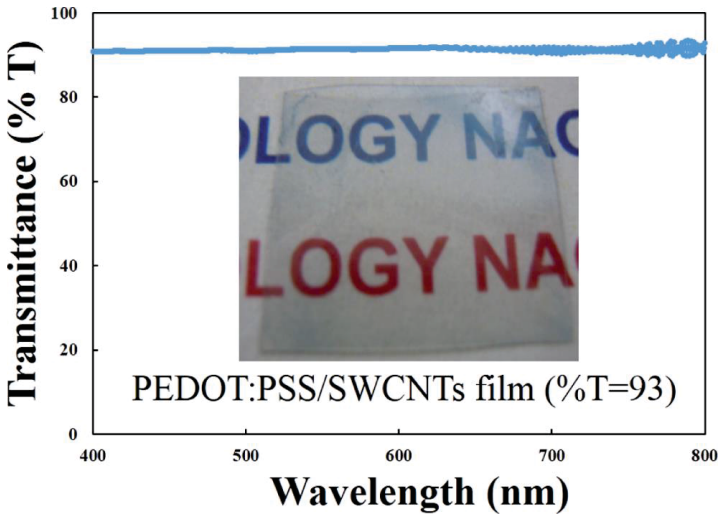

Fig. 4.3 UV–Vis spectrum of the PEDOT:PSS/SWCNTs film fabricated on PET substrate. Inset shows the transparency of the film.

The enhanced conductivity was due to the removal of insulating PSS from the

PEDOT:PSS surface which in turn increased the crystallinity of the film. The detailed mechanism of the conductivity enhancement of the PEDOT:PSS film was described elsewhere [17]. The addition of SWCNTs on the PEDOT:PSS surfaces did not change the conductivity of the film as I used 1 ml of SWCNT solution (concentration 1 mg/40 ml).

4.4 FE study

4.4.1 Schematic of FE setup

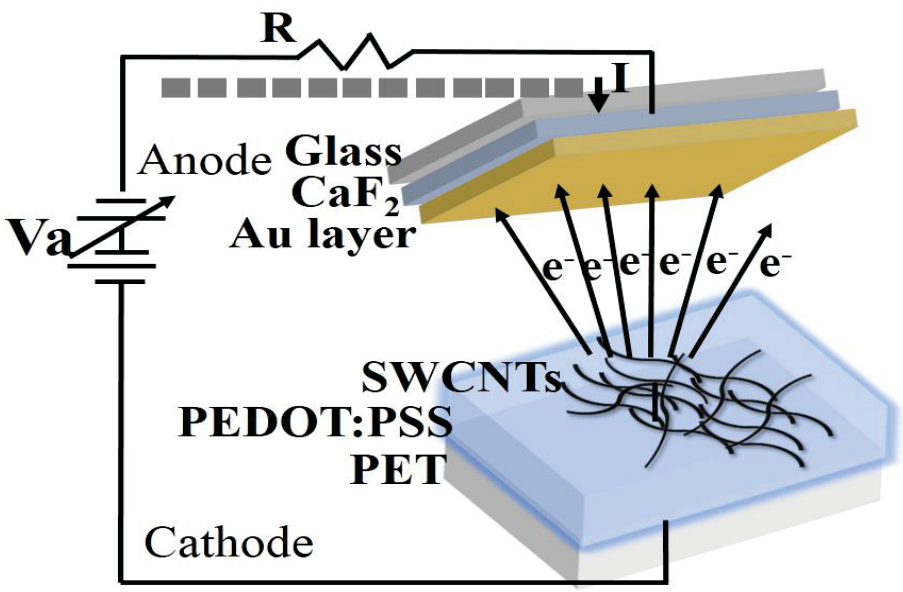

Fig. 4.4 A schematic diagram of CNT based FEDs: PEDOT:PSS/SWCNTs hybrid film was used as a cathode material and ITO glass used as anode material and for light emission image gold coated CaF_2 was used as anode material.

The detailed experimental setup for FEDs was described in the Chapter 2. Here

I used PET space between the cathode and anode. The SWCNTs and PEDOT:PSS/SWCNTs based materials were used as cathode materials and indium tin oxide (ITO) was used as an anode material. For light emission image, I used Au coated on CaF2 phosphor material as a screen. The schematic diagram of FEDs including cathode and anode material is shown in Fig. 4.4.

4.4.2 FE property of PEDOT:PSS film

The FE properties of the PEDOT:PSS film are also shown in Fig. 4.5, revealing that almost no FE occurred. This is due to the fact that there is no emission tip in PEDOT:PSS. However, the combination of PEDOT:PSS film and SWCNTs showed better FE properties than the SWCNTs film alone. The high conductivity of PEDOT:PSS would continuously supply electrons to SWCNTs.

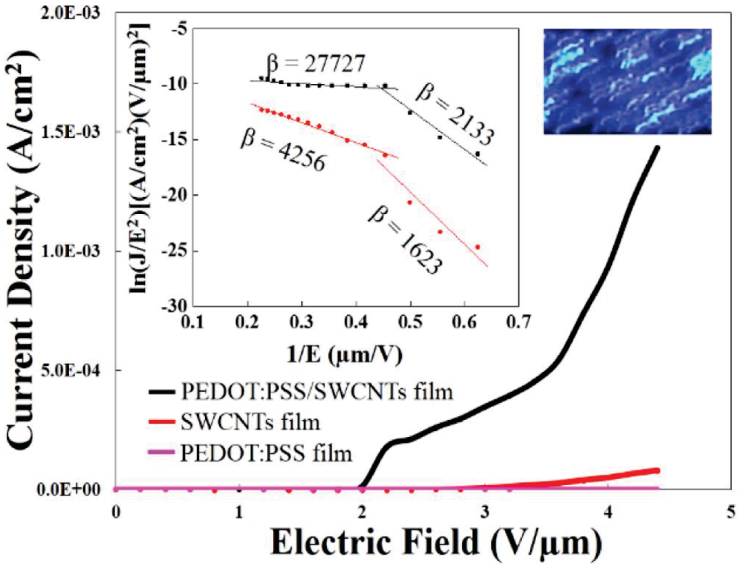

Fig. 4.5 FE curves of PEDOT:PSS/SWCNTs, SWCNTs and PEDOT:PSS films on PET substrate. Left inset: F-N plot of PEDOT:PSS/SWCNTs (black) and SWCNTs film (red) on PET and the corresponding β values in two different regions. Right inset: Emission image of the hybrid structure.

4.4.3 FE comparison of SWCNTs and PEDOT:PSS/SWCNTs film

The FE performance of the films is shown in Fig. 4.5. The turn-on and the threshold field of the SWCNTs film were 2.02 V/μm and 2.38 V/μm, respectively. The PEDOT:PSS/SWCNTs film showed a turn-on field of 0.95 V/μm for the current density of 10 nA/cm^2. The threshold field, that can be defined as to extract the current density 1 μA/cm^2, was found to be 1.77 V/μm. This result indicates that PEDOT:PSS plays a key role for the enhancement of FE performance. The left inset of Fig. 4.5 shows the F-N plot for the SWCNTs and the PEDOT:PSS/SWCNTs film. The straight-line nature in the F-N plot suggests that FE characteristic follows through the tunneling of electrons across

the potential energy barrier. The right inset shows the light-emission image of the hybrid structure using gold coated CaF_2 as an anode material.

By plotting the slopes in two different regions of the F-N curve and assuming a constant $B = 6.83 \times 10^3$ $eV^{-3/2}$ V μm^{-1} and taking the value of work function of SWCNTs as 5.00 eV, I can calculate the β. The FE characteristic follows the F-N plot through the tunneling of cold electrons into the vacuum. The F-N plot shows two parts, i.e., for low and high electric fields. The behavior in the high electric field region may be due to space charge effects [18]. The β values are in the order of 2133 and 27727 in the low and high electric field regions, respectively, for the PEDOT:PSS/SWCNTs hybrid film as shown in Fig. 4.5.

The first report of FE properties of regioregular poly-(3-octylthiophene) deposited on n-doped silicon substrate was developed by Musa et al. [19]. Lai reported the FE properties of the conducting polymer polyaniline doped with camphor sulfonic acid by changing the surface using the electric discharge method [20].

FE occurs by extraction of electrons from the conducting solid under the presence of electric field. High electric field is required for tunneling of electrons and it must overcome the potential barrier. The electrons tunnel easily through the potential barrier and consequently the FE properties are also increased in the hybrid

PEDOT:PSS/SWCNTs structure.

Recently, my group fabricated fully flexible and transparent FEDs based on metavanadate phosphor coated on SWCNT network with turn-on and threshold fields of 5.6 V/μm and 8.8 V/μm, respectively [21]. The turn-on and threshold fields of PEDOT:PSS/SWCNTs were better than for SWCNTs based transparent and flexible film fabricated on PET substrate. Lahiri et al. reported the transparent and flexible FEDs using the hybrid structure of graphene and CNTs as a cathode and phosphor coated on graphene as an anode material with turn-on and threshold fields of 2.05 V/μm and 2.2 V/μm, respectively [10]. My hybrid structures showed better FE performance compared to graphene and CNT based hybrid structure [10].

4.5 Conclusion

Highly efficient and superior transparent and flexible FEE has been developed by simple drop casting followed by spray coating method. The superior FE properties of the PEDOT:PSS were achieved by coating SWCNTs on top of the conducting polymer surface. The sheet resistance of the PEDOT:PSS film was 3.5 kΩ/sq at 93% transparency. The turn-on and threshold fields of SWCNTs and PEDOT:PSS/SWCNTs were observed to be 2.02, 2.38 V/μm and 0.95, 1.77 V/μm, respectively. Interestingly, this hybrid structure showed a very high current density (10^{-3}A/cm^2) at very low electric field. This

conductive polymer based PEDOT:PSS/SWCNTs hybrid structure could be helpful to fabricate future rollable, portable, transparent and flexible FEDs.

4.6 References

[1] S. R. P. Silva, J. D. Carey, G. Y. Chen, D. C. Cox, R. D. Forrest, C. H. Poa, R. C. Smith, Y. F. Tang and J. M. Shannon, PIEE Circuits Devices and Systems, **151**, 489-514 (2004).

[2] S. Itoh, M. Tanaka, and T. Tonegawa, J. Vac. Sci. Technol. B, **22**, 1362-1366 (2004).

[3] X. Guo, and S. R. P. Silva, IEEE Electron Device Lett. **28**, 710-712 (2007).

[4] P. Ghosh, S. Satou, T. Tsuchiya, Y. Hayashi, and M. Tanemura, Phys. Status Solidi RRL **6**, 184-186 (2012).

[5] D. Ghosh, P. Ghosh, M. Tanemura, A. Haysahi, Y. Hayashi, K. Shinji, N. Miura, M. Z. Yusop, and T. Asaka, Chem. Commun. **47**, 4980-4982 (2011).

[6] Y. Guo, H. Liu, Y. Li, G. Li, Y. Zhao, Y. Song, and Y. Li, J. Phys. Chem. C, **113**, 12669-12673 (2009).

[7] S. Y. Lee, C. Jeon,Y. Kim, W. C. Choi, K. Ihm, T.-H. Kang, Y.-H. Kim, C. K. Kim, and C.-Y. Park, Appl. Phys. Lett. **100**, 023102-3 (2012).

[8] Z. Ni, A. Ishaq, L. Yan, J. Gong, and D. Zhu, J. Phys. D: Appl. Phys. **42**, 075408-4 (2009).

[9] Y. Zou, P. W. May, S. M. C. Vieira, and N. A. Fox, J. Appl. Phys. **112**, 044903-5 (2012).

[10] I. Lahiri, V. P. Verma, W. Choi, Carbon. **49**, 1614-1619 (2011).

[11] J. O. Hwang, D. H. Lee, J. Y. Kim, T. H. Han, B. H. Kim, M. Park, K. No, and S. O. Kim, J. Mater. Chem., **21**, 3432-3437 (2011).

[12] D. J. Lipomi, J. A. Lee, M. Vosgueritchian, B. C.-K. Tee, J. A. Bolander, and Z. Bao, Chem. Mater. **24**, 373−382 (2012).

[13] Y. Xia, K. Sun, and J. Ouyang, Energy Environ. Sci. **5**, 5325-5332 (2012).

[14] B. Lee, V. Seshadri, and G. A. Sotzing, Langmuir **21**, 10797-10802 (2005).

[15] X. Crispin, F. L. E. Jakobsson, A. Crispin, P. C. M. Grim, P. Andersson, A. Volodin, C. van Haesendonck, M. Van der Auweraer, W. R. Salaneck, and M. Berggren, Chem. Mater. **18**, 4354-4360 (2006).

[16] M. Vosgueritchian, D. J. Lipomi, and Z. Bao, Adv. Funct. Mater. **22**, 421-428 (2012).

[17] J. Ouyang, Q. Xu, C. W. Chu, Y. Yang, G. Li, and J. Shinar, Polymer **45**, 8443-8450 (2004).

[18] M.-C. Lin, J. Vac. Sci. Technol. B. **25**, 493-496 (2007).

[19] I. Musa, D. A. I. Munindrasdasa, G. A. J. Amaratunga, and W. Eccleston, Nature **395**, 362-365 (1998).

[20] G. Lai, Z. Li, L. Cheng, and J. Peng, J. Mater. Sci. Technol. **22**, 677-680 (2006).

[21] D. Ghosh, P. Ghosh, M. Z. Yusop, M. Tanemura, Y. Hayashi, T. Tsuchiya, and T. Nakajima, Phys. Status Solidi RRL **6**, 303-305 (2012).

Chapter 5

Highly transparent and flexible field electron emitters based on hybrid carbon nanostructure

5.1 Introduction

CNTs have been widely used in various fields such as transparent and flexible FEDs [1], scanning probes [2], solar cells [3], transistors [4] and supercapacitors [5] etc. for their extraordinary electronic and mechanical properties [6-7]. CNTs are very effective for FEDs due to their sharp emission tips and high aspect ratio [8-11]. Materials such as CNCSs [12], graphene [13-16], and ZnO based nanostructures [17-20] are effective to act as FEE. Transparent and flexible FEE have been studied by vertical ZnO nanowire/graphene [21], and metallic nanowire/grapheme [22] based structures. Carbon based hybrid structures might be helpful to enhance the FE device performances and might act as a better cathode material than individual nanostructures [23-26].

Recently, carbon based transparent and flexible FEE of graphene with MWNTs have been reported [27]. In my recent reports, I used a very straightforward method of the random networks of SWCNTs on flat polymer substrates to fabricate transparent and flexible FEE [28]. Recent reports have been focused on the fabrication of CNCSs on nafion substrate at room temperature [29-30]. The low transmittance of the CNCSs and high turn-on and threshold field were major drawback towards the fabrication of transparent and flexible FEEs. Replacing the metal layer by the other transparent materials onto the CNCSs surface could be very interesting to enhance the FEE

performance and the transparency of the device. However, the controlled growth of the hybrid nanostructure on heat sensitive substrate is challenging task and here in this Chapter, I overcome the problem using room temperature growth method and followed by spray coating method.

5.2. Experimental details

5.2.1 Fabrication of the CNCSs on nafion surface

In this Chapter, I fabricated the CNCSs on transparent and flexible nafion substrate at room temperature for the development of transparent and flexible FEDs. The nafion substrate of size 1.5mm×1.5 mm and thickness 100 μm was used for the room temperature growth of the CNCSs. A Kaufman type ion gun (ION TECH.INC.Ltd., model 3-1500-100 Fc) was used with Ne^+ as ion source for the fabrication of the CNCSs during the ion beam irradiation.

5.2.2 Fabrication of the hybrid film

The fabrication of SWCNTs film onto plastic was described in the Chapter 2. I prepared six different kinds of thin films from 0.5, 1 to 1.5 ml SWCNTs solution on both CNCSs and nafion surfaces at the same condition. The distance between the samples and the nozzle of the spray coater was 20 cm and the gas pressure was fixed at 0.5 MPa.

5.3 Results and discussion

5.3.1 Morphology of the hybrid carbon nanostructure film

Fig. 5.1a and 5.1b show the FESEM images of CNCSs coated by 1.5 ml and 0.5 ml SWCNTs solution respectively. It can be observed that the SWCNTs were randomly oriented onto the CNCSs surface in both cases.

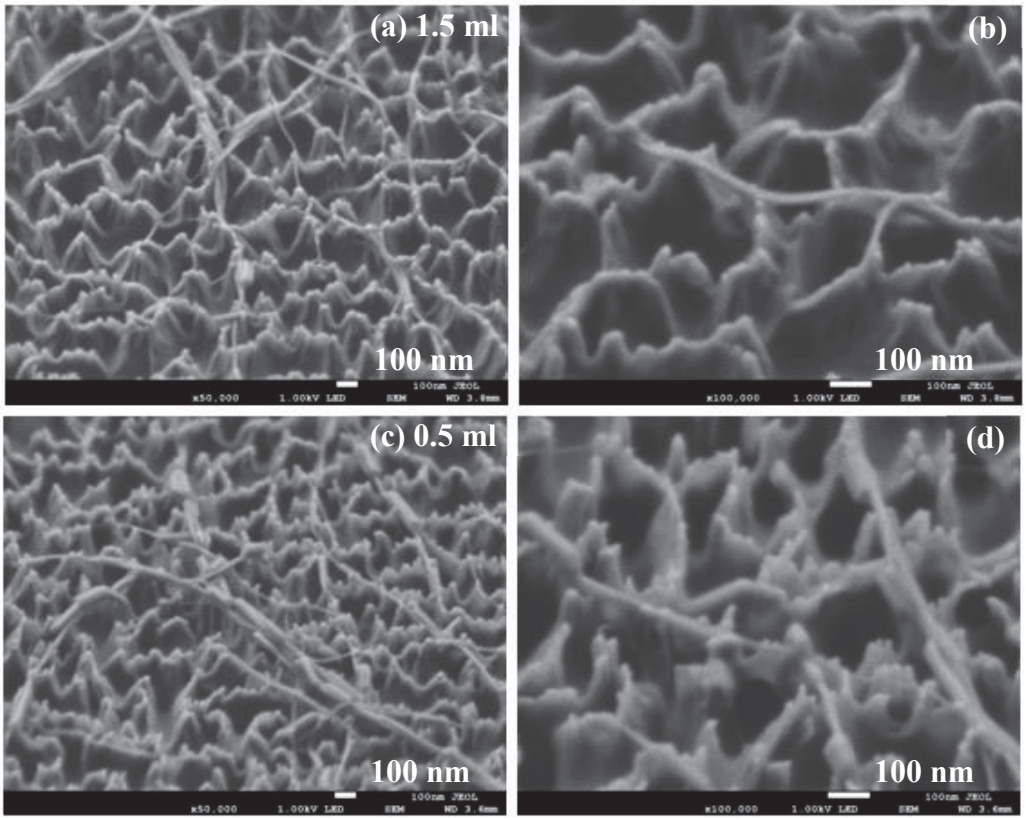

Figure 5.1 FESEM images of SWCNTs coated CNCSs substrate with different SWCNTs amount (a) (b) 1.5 and (c) (d) 0.5 ml. Images in the left side were at 50000× and on the right side were at 100000× magnification.

The morphology of SWCNTs for 1.5 ml on CNCSs surfaces was higher than 0.5 ml SWCNTs. Such kind of random morphology is very much favorable for FEE as the

screening effect is absent.

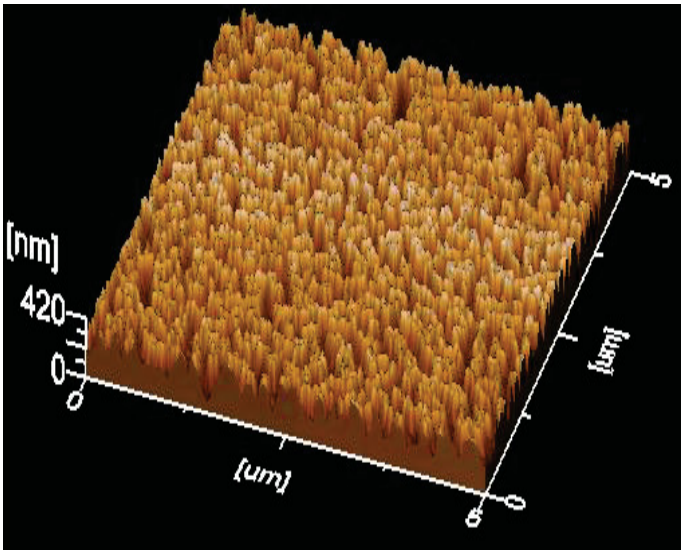

Fig. 5.2 A typical AFM image of CNCSs fabricated on nafion substrate.

A typical AFM image was performed to describe the morphology of CNCSs, shown in Fig. 5.2. The diameter and the length of these CNCSs are 200 nm and 160 nm respectively. Here, I irradiated nafion substrate by Ne^{+} ion for very short irradiation time (10 sec). Increasing the irradiation time the length and the diameter of CNCSs are also changed.

The UV-Vis spectrum of SWCNTs coated nafion and CNCSs were shown in Fig. 5.3.

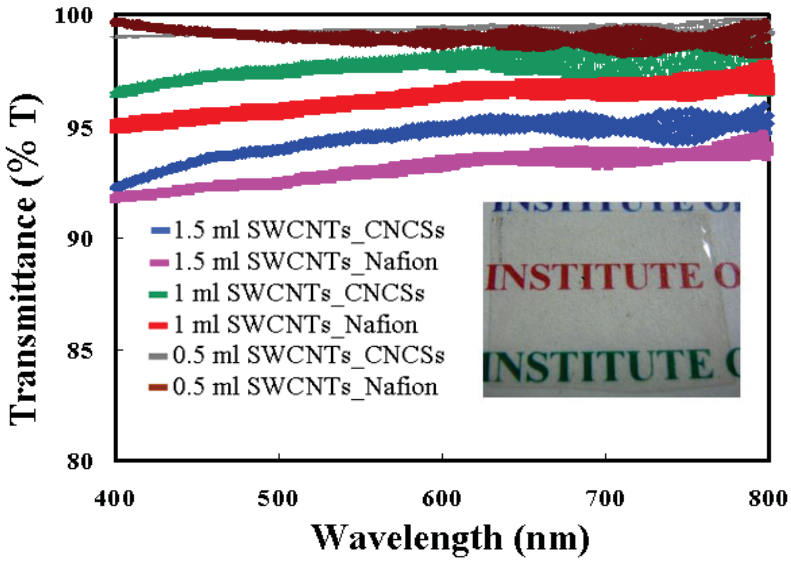

Fig. 5.3 UV-Vis spectrum of CNCSs and bare nafion substrates coated by different amount of SWCNTs from 0.5 to 1.5 and inset shows the transparency of CNCSs film coated by 1 ml SWCNTs solution.

At 550 nm, the transparencies of CNCSs (1.5 ml) and flat nafion (1.5 ml) surfaces are 94.48% and 92.88% respectively. The transparency of CNCSs based thin film showed higher than bare nafion film at the same concentration of SWCNTs. This is due to the controlling the diameter of CNCSs in nanometers region by tuning its refractive index to increase the antireflective properties. To maintain the good transparency of the film, I used very small amount of SWCNTs solution on both bare nafion and CNCSs surfaces. The sheet resistances of these films were found to be 570 kΩ/sq. The diameter of these SWCNTs was measured by a HRTEM shown in figure 5.4.

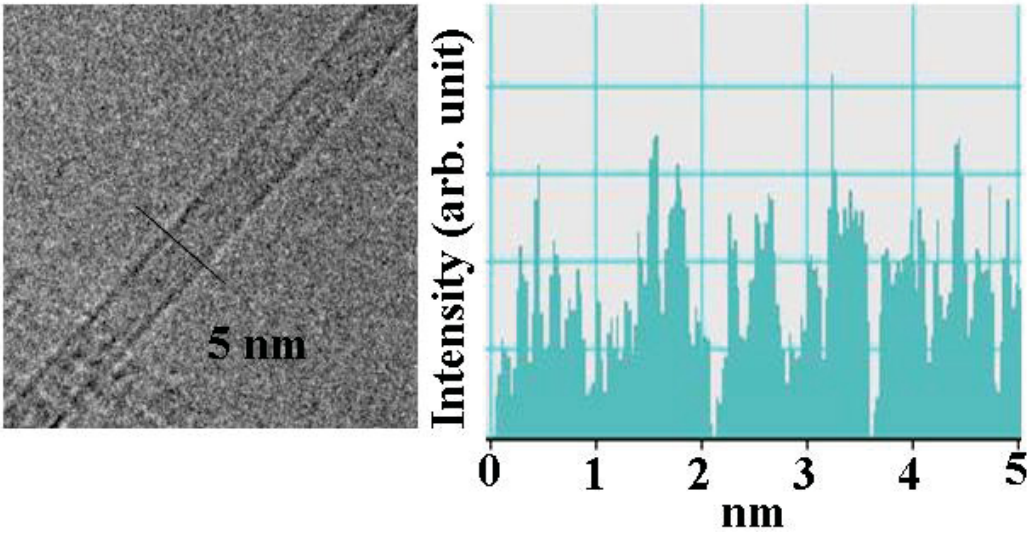

Fig. 5.4 (a) HRTEM image of an individual SWCNT (b) intensity profile of an isolated SWCNT along the line.

The diameter of the individual SWCNTs was found to be 1.5 nm.

5.3.2 FE study of the hybrid carbon nanostructure film

Fig. 5.5 shows the FEE characteristic behavior of CNCSs and nafion substrate coated by SWCNTs. The values of different turn-on and threshold field are summarized in table 1. The turn-on field defined as the fields required to extract the current density 1 nA/cm^2 decreased from CNCSs to nafion substrate at same SWCNTs solution. Similarly the threshold field also defined as the fields required to extract the current density 0.1 μA/cm^2. From the FE result, it was confirmed that SWCNTs coated CNCSs showed much better FE properties than flat nafion, due to extra emission sites. The CNCSs surface covered randomly by SWCNTs and it occupies the position of top of the CNCSs. All the CNCSs are not covered by SWCNTs, the remaining CNCSs that are not covered by

SWCNTs do not show FE properties. The junction where the SWCNTs and CNCSs are combined, FE occurs from both CNCSs and SWCNTs. There is decreased of FE properties from 1.5 ml to 0.5 ml SWCNTs on CNCSs surfaces which is shown in Table 1.

Table 1 Parameters describing the FE properties of CNCSs and nafion film coated by different amount of SWCNTs solution

SWCNTs amount (ml)	Substrates	Turn-on field (V/μm)	Threshold field (V/μm)
1.5	CNCSs	2.08	3.00
1.5	nafion	3.25	3.73
1.0	CNCSs	2.84	3.53
1.0	nafion	3.86	4.29
0.5	CNCSs	2.70	3.84
0.5	nafion	2.27	5.14

Interestingly, the FE properties on CNCSs (0.5 ml) and bare nafion (1.5 ml) substrate are nearly equal which are shown in Fig. 5.5. SWCNTs are randomly oriented for 0.5 ml solution on CNCSs surface. In bare nafion surface coated by 1.5 ml, only SWCNTs act as FEE. CNCSs (0.5 ml) surface showed better FE properties than bare nafion (1 ml) surface. From these results, I can conclude that CNCSs might act as a suitable cost-effective cathode material for FEDs. The FE performance decreased from 1.5 ml to 0.5 ml SWCNTs solution on CNCSs surfaces due to the fewer number of

emitters available on the combined structures.

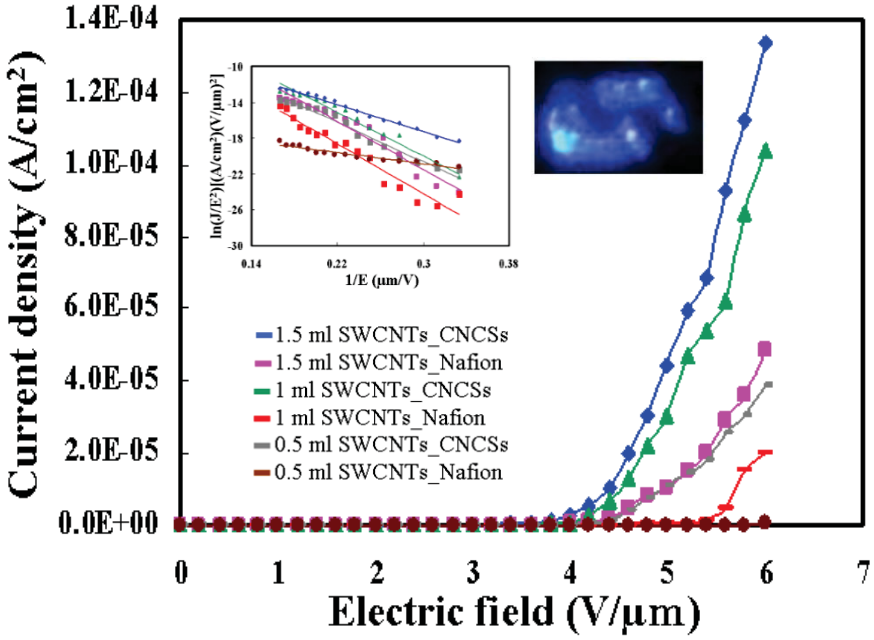

Fig. 5.5 FE curves of SWCNTs/CNCSs and SWCNTs/nafion substrate coated by different amounts of SWCNTs solution. Left inset shows F-N plot of CNCSs-SWCNTs and CNCSs-nafion substrate coated by different amounts of SWCNTs solution and the right inset shows the light emission image of SWCNTs/CNCSs hybrid structure.

The FE properties of SWCNTs/CNCSs and SWCNTs/nafion substrate are shown in Fig. 5.5. The inset of Fig. 5.5 shows the F-N plot for SWCNTs/CNCSs and SWCNTs/nafion films. It can be corroborated that the emission characteristics of these samples follow F-N plot.

I have fabricated the transparent and flexible FEE using the random networks of SWCNTs with maximum current density ~6×10^{-5}A/cm^2 at 5 V/μm [28]. Verma et al.

reported the FE of graphene PET substrate with excellent emission properties [31]. The transparency of the graphene/PET film was found to be 88.88%. Although the graphene based PET film showed higher FE than my results, but from the viewpoint of transparency, my hybrid carbon nanostructure based film much better than grapheme/PET film.

Recently, SnO_2, BN and AlN nanocone fabricated on rigid substrate and show excellent FE properties with low operating voltage [32-34]. So far, only few reports have been devoted using CNCSs as transparent and flexible FEE. My groups have been studied Au coated CNCSs on transparent and flexible nafion substrate with turn-on and threshold field 6.1 and 9.5 V/μm respectively [29]. Recently, researchers fabricated the CNCSs on nafion substrate and studied the FE properties of Pt coated CNCSs surfaces with turn-on and threshold field 6.4 and 6.7 V/μm respectively which was much higher than these results [30]. SWCNTs/CNCSs hybrid structures showed much better FE properties than SWCNTs, Pt or Au coated CNCSs. The emission properties of 1 ml SWCNTs on CNCSs are slightly decreased than 1.5 ml SWCNTs on CNCSs although the transparency is also increased from 1.5 ml to 1 ml SWCNTs solution on CNCSs surfaces. The transparency and FE properties were competing with each other. Thus from the viewpoint of transparency and FE properties, CNCSs (1 ml) are the best candidate in my case to develop transparent and flexible FEE.

5.4 Conclusion

In conclusion, I have demonstrated a cost-effective technique for the fabrication of transparent and flexible FEE based on SWCNTs and CNCSs hybrid structure. The FE properties of these combined structures were dramatically increased compared to either SWCNTs or CNCSs. Various amounts of SWCNTs were coated on CNCSs and nafion surfaces and the FE characteristic were compared. A maximum current density 1.3×10^{-4} A/cm^2 was observed at 5.7 V/μm for 1.5 ml SWCNTS solution on CNCSs surface. SWCNTS/CNCSs based hybrid film showed high transparency (~ 95%) in the visible wavelength. Thus the fabrication of room temperature growth of the hybrid structure (SWCNTs/CNCSs) could pave the way to develop transparent and flexible FEDs in near future.

5.5 References

[1] D. Ghosh, P. Ghosh, M. Z. Yusop, M. Tanemura, Y. Hayashi, T. Tsuchiya, and T. Nakajima Phys. Status Solidi RRL, **6,** 303-305 (2012).

[2] C. V. Nguyen, Q. Ye and M. Meyyappan, Meas. Sci. Technol. **16,** 2138-2146 (2005).

[3] Y. Jung, X. Li, N. K. Rajan, A. D. Taylor, and M. A. Reed, Nano Lett. **13,** 95-99 (2013).

[4] S. Aikawa, E. Einarsson, T. Thurakitseree, S. Chiashi, E. Nishikawa, Appl. Phys. Lett. **100,** 063502-4 (2012).

[5] B. Kim, H. Chung and W. Kim, Nanotechnology **23,** 155401-8 (2012).

[6] M. Ouyang, J.-L. Huang, and C. M. Lieber, Acc. Chem. Res. **35,** 1018-1025 (2002).

[7] M. Cadek, J. N. Coleman, V. Barron, K. Hedicke, and W. J. Blau, Appl. Phys. Lett. **81,** 5123-5125 (2002).

[8] T. Kuzumaki, Y. Takamura, H. Ichinose, and Y. Horiike, Appl. Phys. Lett. **78,** 3699-3701 (2001).

[9] C L. Pint, S. T Pheasant, M. Pasquali, K. E. Coulter, H. K. Schmidt, and R. H. Hauge, Nano Lett. **8,** 1879-1883 (2008).

[10] G. Chen, D. H. Shin, S. Roth, and C. J. Lee, Nanotechnology **20,** 315201-5 (2009).

[11] Y. Saito, Y. Tsujimoto, A. Koshio, and F. Kokai, Appl. Phys. Lett. **90,** 213108-3

(2007).

[12] Q. Z. Zhao, F. Ciobanu, and L. J. Wang, Appl. Phys. Lett. **105,** 083103-4 (2009).

[13] Z.-S. Wu, S. Pei, W. Ren, D. Tang, L. Gao, B. Liu, F. Li, C. Liu, and H.-M. Cheng Adv. Mater. **21,** 1756-1760 (2009).

[14] W. Lei, C. Li, M. T. Cole, K. Qu, S. Ding, Y. Zhang, J. H. Warner, X. Zhang, B. Wang, W. I. Milne, Carbon **56,** 255-263 (2013).

[15] Y. Guo, W. Guo, J. Phys. Chem. C **117,** 692-696 (2013).

[16] Z. Xiao, J. She, S. Deng, Z. Tang, Z. Li, J. Lu, and N. Xu, **4,** 6332-6336 (2010).

[17] H. Y. Yang, S. P. Lau, S. F. Yu, L. Huang, M. Tanemura, J. Tanaka, T. Okita, H. H. Hng, Nanotechnology **16,** 1300-1303 (2005).

[18] C. J. Park, D.- K. Choi, J. Yoo, G.- C. Yi, C. J. Lee, Appl. Phys. Lett. **90,** 083107-3, (2007).

[19] C. X. Xu, and X. W. Sun, Appl. Phys. Lett. **83,** 3806-3808 (2003).

[20] D. Pradhan, M. Kumar, Y. Ando, and K. T. Leung, ACS Appl. Mater. Interfaces **1,** 789-796 (2009).

[21] J. O. Hwang, H. D. Lee, J. Y. Kim, T. H. Han, B. H. Kim, M. Park, K. No, and S. O. Kim, J. Mater. Chem. **21,** 3432-3437 (2011).

[22] M. Arif, K. Heo, B. Y. Lee, J. Lee, D. H. Seo, S. Seo, J. Jian, and S. Hong,

Nanotechnology **22,** 355709-7 (2011).

[23] X. Xiao, O. Auciello, H. Cui, D. H. Lowndes, V. L. Merkulov, J. Carlisle, Diamond Relat. Mater. **15,** 244-247 (2006).

[24] Y. Guo, H. Liu, Y. Li, G. Li, Y. Zhao, Y. Song, and Y. Li, J. Phys. Chem. C **113,** 12669-12673 (2009).

[25] D. H. Lee, J. A. Lee, W. J. Lee, D. S. Choi, W. J. Lee, and S. O. Kim, J. Phys. Chem. C **114,** 21184-21189 (2010).

[26] Y. M. Ho, G. M. Yang, W. T .Zheng, X. Wang, H. W. Tian, Q. Xu, H. B. Li, J. W. Liu, J. L. Qi, and Q. Jiang, Nanotechnology **19,** 065710-6 (2008).

[27] I. Lahiri, V. P. Verma, W. Choi, Carbon **49,** 1614-1619 (2011).

[28] D. Ghosh, P. Ghosh, M. Tanemura, A. Haysahi, Y. Hayashi, K. Shinji, N. Miura, M. Z. Yusop, and T. Asaka, Chem. Commun. **47,** 4980-4982 (2011).

[29] P. Ghosh, M. Z. Yusop, S. Satoh, M. Subramanian, A. Hayashi, Y. Hayashi, and M. Tanemura, J. Am. Chem. Soc. **132**, 4034-4035 (2010).

[30] P. Ghosh, S. Satou, T. Tsuchiya, Y. Hayashi, and M. Tanemura, Phys. Status Solidi RRL **6,** 184-186 (2012).

[31] V. P. Verma, S. Das, I. Lahiri, and W. Choi, Appl. Phys. Lett. **96,** 203108-3 (2010).

[32] X. – B. Li, X.- W. Wang, Q. Shen, J. Zheng, W.- H. Liu, H. Zhao, F. Yang, and H.-

Q. Yang, ACS Appl. Mater. Interfaces **5,** 3033-3041 (2013).

[33] W. An, X. Wu, X. C. Zeng, J. Phys. Chem. B **110,** 16346-16352 (2006).

[34] N. Liu, Q. Wu, C. He, H. Tao, X. Wang, W. Lei, and Z. Hu, ACS Appl. Mater. Interfaces **9,** 1927-1930 (2009).

Chapter 6

Conclusion and future works

6.1 Overall Conclusion

The goal for my research work has been to develop fundamental components necessary to achieve transparent and flexible FEDs on polymer substrates using room temperature growth process.

We have developed and demonstrated transparent and flexible display based on carbon nanomaterials. An ideal SWCNTs based electrode must be highly transparent to allow the maximum amount of light through, and it must also be conductive to provide uniform electrical current distribution. In Chapter 2, a spray coating method was performed to develop the transparent and flexible cathode for FEDs. Transparent and flexible electrode has been fabricated successfully of SWCNTs based highly transparent (transparency = 86%), flexible FEE with turn-on and threshold fields of 2.8 and 4.2 V μm^{-1}, respectively. The data suggests that the SWCNTs based film is better in all of the vital aspects, including transparency, conductivity and FE performance. These SWNTs films with excellent FE properties are expected to have broad implications for the development of next-generation rollable and lightweight displays, with minimized device-to-device variation and enhanced stability.

The most widely used anode in FEDs is tin-dope indium oxide, commonly referred as ITO. Even though ITO has demonstrated good performance as anode for FEDs,

it may not be the best choice for future low-cost and high performance optoelectronic applications in terms of the cost, chemical and mechanical properties of the material. In Chapter 3, $CsVO_3$ is considered to be a promising phosphor as replacement of ITO and was fabricated directly on SWCNT/arylite-based conductive, flexible and highly transparent substrate. SWCNT-based emitters and screen exhibit optical transmission of 92.6% and 54%, respectively. FE measurements indicated that SWCNT-based films are quite effective emitters and produce significant amount of current density. Moreover, it has been demonstrated that our transparent and flexible film is mechanically more stable than the ITO electrode in flexible applications.

In Chapter 4, highly efficient and superior transparent and flexible FEE has been developed by simple drop casting followed by spray coating method. The superior FE properties of the PEDOT:PSS were achieved by coating SWCNTs on top of the conducting polymer surface. This hybrid structure showed a very high current density (10^{-3}A/cm^2) at very low electric field. This conductive polymer based PEDOT:PSS/SWCNTs hybrid structure could be helpful to fabricate future rollable, portable, transparent and flexible FEDs.

In Chapter 5, I have demonstrated a cost-effective technique for the fabrication of transparent and flexible FEE based on SWCNTs and CNCSs hybrid structure. The FE

properties of these combined structures were dramatically increased compared to either SWCNTs or CNCSs. A maximum current density 1.3×10^{-4}A/cm^2 was observed at 5.7 V/μm for 1.5 ml SWCNTS solution on CNCSs surface. The hybrid structure (SWCNTs/CNCSs) could pave the way to develop transparent and flexible FEDs in near future.

I have proposed a scheme for the development of transparent and flexible FEDs, there are some limitations from material to device.

The fabrication of cathode material over large-area, stable and uniform emission properties is required. The suitable low voltage phosphor material is required on transparent, flexible and conductive substrate to realize the transparent and flexible FEDs in near future. Large scale fabrication of the material over large area on polymer substrate at room temperature is required. And finally, vacuum level should be maintained, spacer affects the image quality so the proper selection of the spacer is also important. The present experimental data could be helpful in near future to fabricate the transparent and flexible FEDs.

6.2 Future research work

Nowadays transparent, conductive and flexible electrodes are necessary components for many transparent and flexible device applications such as OLEDs, FEDs etc. The realization of cost-effective transparent and conductive electrodes is the key to achieve these displays.

The Ag nanoparticles based thin film showed outstanding conductive and transparent properties (9 Ω/sq at 75T). The properties of Ag nanoparticles based thin film are very close to ITO and CNTs based electrode. These outstanding properties of Ag nanoparticles based thin film might be interesting to replace the very well-known expensive electrodes based on CNTs electrode. Proper alignment of Ag nanoparticles is very important to realize the efficient transparent and flexible cathode material for FEDs. In this regard, the ripple structure might be helpful to align the Ag nanoparticles.

We fabricated the ripple structure on flexible polymer substrate using ion beam irradiation by room temperature method. The fabrication of this ripple structure formed on polymer substrates without affecting the transparency. The proper alignment of Ag nanoparticles on ripple structure could be helpful to tune transparency and conductivity. The period and the amplitude of this ripple structure is 100 and 70 nm respectively. To align the Ag nanoparticles on the ripple structure, the diameter of the Ag nanoparticles is

very important. The transparent, conductive and flexible electrode based on Ag nanoparticles on ripple structures could be beneficial to fabricate the future bendable, rollable transparent and flexible devices. These outstanding properties of Ag nanoparticles based thin film might be interesting to replace the very well-known expensive electrodes based on SWCNTs.

Acknowledgements

It is always great pleasure to acknowledge those who made the thesis possible. First, I would like to convey my sincere gratitude to my Prof. Masaki Tanemura for giving me the opportunity in his laboratory. I would also like to express my gratitude and earnest thanks to my supervisor Prof. Masaki Tanemura, whose constant encouragement, patience and sustained guidance has made this thesis comes true.

I would like to thank Prof. T. Soga and Prof. T. Hihara for an improvement of the thesis. I would also like to thank Prof. Yasuhiko Hayashi for his useful suggestions and encouragements. I would like to thank Dr. Pradip Ghosh, Dr. Golap Kalita, and Dr. M. Subramanian for their help, discussion and critical comments during my study. I am also grateful to thank all of my laboratory members for their kind support and help.

I wish to express my immense gratitude to my parents for their constant encouragement and moral support. Finally, I am grateful to thank all of my research staffs in my laboratory.

I would like to acknowledge Nikki Saneyoshi, Japan student services organization (JASSO) scholarship foundation and research associate (RA) for international students during the study of my doctor's program. I also would like to thank my supervisor Prof. Masaki Tanemura to help financially during my doctor's study.

List of publications

[1] **Debasish Ghosh**, Pradip Ghosh, Masaki Tanemura, Akari Haysahi, Yasuhiko Hayashi, Kawasaki Shinji, Noboru Miura, Mohd. Zamri Yusop and Toru Asaka, "*Highly transparent and flexible field emission devices based on single-walled carbon nanotube films*" **Chem. Commun**., 47, 4980–4982 (2011).

[2] **Debasish Ghosh**, Pradip Ghosh, Mohd. yusop, Masaki Tanemura, Yasuhiko Hayashi, Tomohiko Nakajima, "*Transparent and flexible field emission display device based on single-walled carbon nanotubes*" **Phys. Status Solidi RRL**, 6, 303-305 (2012).

[3] **Debasish Ghosh**, Pradip Ghosh, Golap Kalita, Takuto Noda, Chisato Takahashi, and Masaki Tanemura, "*Conducting polymer based hybrid structure as transparent and flexible field electron emitter*" **Phys. Status Solidi RRL**, 7, 489-492 (2013).

[4] **Debasish Ghosh,** Pradip Ghosh, Takuto Noda, Yasuhiko Hayashi, and Masaki Tanemura "*Transparent and flexible field electron emitter based on hybrid carbon nanostructure*" Under preparation.

[5] Pradip Ghosh, M. Zamri Yusop, **Debasish Ghosh**, Akari Hayashi, Yasuhiko Hayashi, and Masaki Tanemura, "*Direct fabrication of aligned metal composite carbon nanofibers on copper substrate at room temperature and their field emission property*" **Chem. Commun**., 47, 4820–4822, (2011).

[6] Pradip Ghosh, Mohd Zamri, **Debasish Ghosh**, Tetsuo Soga, Takashi Jimbo, Shinobu Hashimoto, Shuho Ohashi, and Masaki Tanemura, "*Improvement in field electron emission performance of natural-precursor-grown carbon nanofibers by thermal annealing in argon atmosphere*" **Jpn. J. Appl. Phys.** 50, 01AF09-4, (2011).

Conference Presentations

[1] Poster presentation "*Fabrication and characterization of conical nanocarbon structures on polymer substrate for transparent and flexible field emission display*" ISPlasma, Nagoya Institute of Technology, Nagoya, Japan, (2011).

[2] Poster presentation "*Development of Carbon Nanostructure based highly Transparent and Flexible Field Emitter*" MNC 2012, 25th International Microprocesses and Nanotechnology Conference, Kobe Merikken Park Oriental Hotel, Kobe, Japan (2012).

[3] Oral presentation "*Development of carbon nanostructure based highly transparent and flexible field electron emitter*" Surface Science Society of Japan (Chubu Branch), Nagoya, Japan (2012).